Editors' Suggestion

Breakdown of the Migdal-Eliashberg theory and a theory of lattice-fermionic superfluidity

Emil A. Yuzbashyan[1] and Boris L. Altshuler[2]

[1]*Department of Physics and Astronomy, Rutgers University, Piscataway, New Jersey 08854, USA*

[2]*Physics Department, Columbia University, 538 West 120th Street, New York, New York 10027, USA*

(Received 10 June 2022; revised 8 August 2022; accepted 9 August 2022; published 24 August 2022)

We show that the Migdal-Eliashberg theory loses validity at a finite value λ_c of the electron-phonon coupling λ regardless of the underlying model Hamiltonian. The value of λ_c is approximately between 3.0 and 3.7. The new phase that emerges at $\lambda > \lambda_c$ breaks the lattice translational symmetry. Depending on the filling fraction and crystal symmetry, it is an insulator or a Fermi liquid. Its characteristic feature is a gap or a pronounced depression of the fermionic density of states near the Fermi level. We establish the breakdown from within the Migdal-Eliashberg theory by demonstrating that the normal state specific heat is negative for $\lambda \geqslant 3.7$ and the quasiparticle lifetime vanishes in the strong coupling limit. At fixed $\lambda > \lambda_c$, the transition to the new phase occurs at a critical temperature higher than the superconducting transition temperature. In addition, there is a first-order phase transition between the new phase and the superconducting state as we vary λ across λ_c at fixed temperature. We put forward a new theory—lattice-fermionic theory of superfluidity—that bridges the gap between the Migdal-Eliashberg approach and the physics at stronger coupling. At small λ, our theory reduces to the Migdal-Eliashberg theory, and past λ_c, it describes the new phase and a range of other phenomena.

DOI: 10.1103/PhysRevB.106.054518

I. INTRODUCTION

Migdal-Eliashberg theory [1,2] is the principal theoretical framework for understanding properties of the normal and superconducting states in metals determined by boson mediated electron-electron interactions. It is a time-dependent mean-field theory that makes accurate quantitative predictions for a wide range of materials of the superconducting transition temperature, quasiparticle gap, and most other thermodynamic and dynamical observables, many of which are beyond the Bardeen-Cooper-Schrieffer (BCS) theory of superconductivity [3]. On a technical level, the Migdal-Eliashberg theory in its simplest formulation comes down to two coupled self-consistency equations, known as the Eliashberg equations, for the normal, $\Sigma(i\omega_n)$, and anomalous, $\Phi(i\omega_n)$, self-energies that are functions of the fermionic Matsubara frequency $\omega_n = \pi T(2n+1)$.

The main open question in the Migdal-Eliashberg theory is its status at strong *renormalized* (actual) electron-phonon coupling λ. This is the question we address in the present paper. We prove that this theory loses validity for $\lambda > \lambda_c$ irrespective of the underlying electron-phonon model, where

$$3.0 \lesssim \lambda_c \lesssim 3.7. \tag{1}$$

The smoking gun evidence of the breakdown is negative specific heat of the Migdal-Eliashberg normal state indicating that it is thermodynamically unstable [4]. Further evidence is the quasiparticle decay rate $\Gamma = \lambda\pi T$ that is much larger than the temperature T at strong coupling and diverges in the limit $\lambda \to \infty$. To address the physics beyond λ_c, we put forward a new theory—lattice-fermionic theory of superfluidity in which the lattice and fermions are closer intertwined. At small λ it reduces to the Migdal-Eliashberg theory and past λ_c it describes the new phase.

We find that it is the interaction of electrons near the Fermi surface mediated by quantum fluctuations of the lattice that makes the specific heat negative within the Migdal-Eliashberg theory. The reason is that this theory misses an abrupt reconstruction of the electronic band structure and formation of new bound states of the low energy electrons and quantum phonons that occur at $\lambda = \lambda_c$. This is assisted by static distortions of the lattice—classical phonons. Such lattice distortions are generally thought to occur at strong electron-phonon interaction [5–11]. We show that they are present already when λ is finite and the Fermi energy is the largest energy scale in the problem. We also find that vanishing of the quasiparticle lifetime in the limit $\lambda \to \infty$ is entirely due to thermal fluctuations of these distortions. At the same time, we will see that quantum rather than classical phonons are the main culprits in the breakdown of the Migdal-Eliashberg theory.

Consider for simplicity the Holstein model of electrons moving on a lattice and interacting with ions. The model assumes ions are independent harmonic oscillators of mass M and spring constant K and takes the Coulomb interaction between electrons and ions to be

$$H_{\text{int}} = \sum_i (\alpha x_i) n_i, \tag{2}$$

where x_i is the displacement of the ion at site i from its equilibrium position and n_i is the number of electrons at this site. The dimensionless electron-phonon coupling constant is defined as

$$\lambda = \frac{\nu_0 \alpha^2}{K}, \tag{3}$$

where ν_0 is the density of electronic states at the Fermi level per lattice site per spin projection. Note that we took K to be the renormalized spring constant.

It is easiest to understand the physics at strong coupling in the limit $\lambda \to \infty$. Equation (3) shows that this is the free ion limit $K \to 0$. The oscillation frequency $\Omega = \sqrt{K/M}$ vanishes together with K. Any finite temperature is much larger than Ω. High-temperature excites lattice oscillators to states with large quantum numbers making them essentially classical (classical phonons). Integrals over momenta of classical oscillators in the partition function decouple from the remaining degrees of freedom. We are left with the kinetic energy of the electrons plus Eq. (2), where x_i are classical variables. The elastic energy $\sum_i K x_i^2/2$ vanishes in the strong coupling limit. The only role of the oscillators now is to provide a statistically distributed on-site potential $V_i = \alpha x_i$ for the electrons. The spatial average of x_i couples to the total electron number only and we absorb it into the chemical potential.

In the mean-field approximation, the problem reduces to finding a nonuniform on-site potential V_i for the electrons that minimizes their free energy. At $K = 0$, the energy can be lowered indefinitely. At $K = \infty$ the only solution is $x_i = 0$, since having nonzero x_i costs infinite elastic energy. As we lower K, at a certain K_c, x_i become nonzero breaking lattice translation symmetry similarly to the Peierls distortion [12,13] and generating a frozen on-site potential $V_i = \alpha x_i$ for the fermions. This potential modifies the fermionic band structure. Since we take the Fermi energy to be much larger than any other characteristic energy, the only possible relevant modification is a pronounced depression of the fermionic density of states near the Fermi level. We show that at least for certain system parameters a hard gap opens triggering a metal-insulator transition.

Migdal-Eliashberg theory assumes translational invariance. For example, electron and phonon Green's functions depend only on coordinate differences. This implies thermal averages of classical ion displacements are zero, $\langle x_i \rangle = 0$. However, fluctuations of x_i are not. $V_i = \alpha x_i$ is then equivalent to disorder potential and thermal averaging to disorder averaging. Using the standard expression for disorder averaged quasiparticle decay rate in a random potential, we find $\Gamma = \lambda \pi T$, which coincides with the prediction of the Migdal-Eliashberg theory.

We see that the divergence of the quasiparticle decay rate in the limit $\lambda \to \infty$ is entirely due to classical phonons. In contrast, negative quasiparticle specific heat cannot be explained in this way. Moreover, we will see that these phonons cancel out from the Migdal-Eliashberg free energy altogether. Therefore, even though classical phonons facilitate the abrupt change in the fermionic band structure, the breakdown of the theory at finite λ occurs only due to strong electron-electron interactions mediated by quantum fluctuations of the lattice, i.e., by quantum phonons.

Above arguments imply that a new order emerges in the electron-phonon system at strong coupling. Fix $\lambda > \lambda_c$. The transition to the new order occurs at a critical temperature T_{c1} above the superconducting transition temperature T_{c2}, since the heat capacity turns negative above T_{c2}. We illustrate this in Fig. 1 where we show schematically the evolution of the free energy profile with T. At very large T, we have a classical gas of electrons and phonons. Below T_{c1} the new phase emerges, which we take to be an insulator for concreteness. At T_{c2} the superconducting stationary point appears, because the nontrivial solution of the Eliashberg equations exists at low enough T for any λ and corresponds to a stationary point of the free energy [14]. Near its inception, the superconducting state is a local minimum or a saddle point, because the insulating minimum is already much below the normal state, see Fig. 1. This means in particular that there is a first-order transition between the superconductor and insulator as a function of λ at temperatures just below T_{c2}.

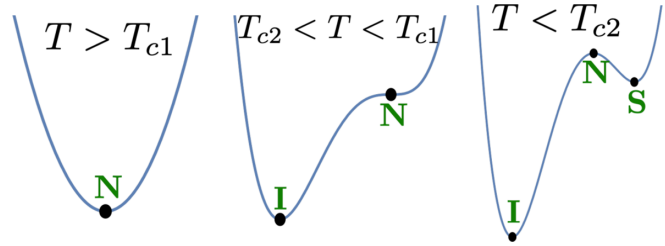

FIG. 1. Free energy profile of the electron-phonon system after the Migdal-Eliashberg theory breaks down, $\lambda > \lambda_c$. New order emerges [insulator (I) in this case] below T_{c1} out of the normal (N) state. Superconducting (S) stationary point appears at a lower temperature T_{c2}. At temperatures just below T_{c2}, this stationary point must be higher in energy than the insulator by continuity.

To describe the entire phase diagram of the electron-phonon system, we propose a new theory, which we dubbed the theory of lattice-fermionic superfluidity. The main idea is to incorporate the classical part of the phonon field into the single-particle Hamiltonian for fermions as an adjustable potential. This generally breaks the lattice translational symmetry. We treat the boson-mediated interaction in particle-particle and particle-hole channels in saddle point approximation as in the Migdal-Eliashberg theory, except now the normal and anomalous self-energies Φ and Σ depend on the single-particle state. The end result is a set of four coupled equations that self-consistently determine classical displacements of the oscillators from their equilibria, single-electron states and energies, and the fields Φ and Σ. This theory reproduces the Migdal-Eliashberg theory at $\lambda < \lambda_c$ and the polaron formation theory [15] in the adiabatic limit $M \to \infty$. It continues to work past λ_c and captures at least some of the new physics that emerges at strong coupling.

In the above discussion, it is crucial to distinguish the *renormalized* electron-phonon coupling λ and the *bare* coupling λ_0. Suppose $\Omega_0 = \sqrt{K_0/M}$ is the bare frequency of Holstein phonons. Migdal and Eliashberg found that within standard electron-phonon models, such as the Frölich or Holstein Hamiltonian, electrons strongly renormalize the phonons, so that the renormalized phonon frequency is [1,2,16],

$$\Omega \approx \Omega_0 \sqrt{1 - 2\lambda_0}. \tag{4}$$

This formula predicts a lattice instability at $\lambda_0 \approx 0.5$ (lattice vibration frequencies become imaginary) restricting the

domain of applicability of the Migdal-Eliashberg theory to $0 \leqslant \lambda_0 \lesssim 0.5$, as Migdal and Eliashberg both note [1,2,17]. Their conclusion that the theory does not work for $\lambda_0 \gtrsim 0.5$ has since been verified and elaborated upon by many other studies [5–11]. However, it is important to emphasize that this does not necessarily violate Migdal's theorem [1,2], which says that quadratic fluctuations of the fermionic fields Σ and Φ around the Eliashberg minimum of the free energy (point S in Fig. 1) are small as long as the Fermi energy is sufficiently large [18]. We just have to keep in mind that this theorem applies only at the Eliashberg stationary point and not at other points, such as the insulating minimum I in Fig. 1. Because of the above lattice instability, one of the main assumptions of the theory as formulated by Migdal and later Eliashberg is that λ_0 is smaller than and not too close to 0.5, see also p. 182 of Ref. [16]. This point is often overlooked in the literature and attempts are made to study the Migdal-Eliashberg theory outside of this interval of λ_0. The finding that the theory does not work for such λ_0 is not news, but was known already to Migdal and Eliashberg.

The true question therefore is not whether the theory stops working beyond $\lambda_0 \approx 0.5$, but if there is an upper bound on the *renormalized* electron-phonon coupling λ. In terms of the electron-phonon interaction energy constant, $g^2 = \nu_0 \alpha^2 M^{-1}$, the renormalized coupling (3) reads $\lambda = g^2/\Omega^2$. Similarly, the bare electron-phonon coupling is $\lambda_0 = g^2/\Omega_0^2$. Equation (4) then implies

$$\lambda = \frac{\lambda_0}{1 - 2\lambda_0}. \tag{5}$$

We see that λ varies from 0 to $+\infty$ within the domain of applicability, $0 \leqslant \lambda_0 \lesssim 0.5$, of the Migdal-Eliashberg theory. This seems to suggest that arbitrarily large values of λ are attainable [19]. Since at strong coupling $T_c/\Omega \approx 0.183\sqrt{\lambda}$ [20], this would imply unbounded T_c in units of the characteristic phonon frequency.

About a decade after Migdal's work Brovman and Kagan realized that the above lattice instability is in fact merely an artifact of conventional electron-phonon models [21,22]. Such models postulate certain lattice vibration spectra, e.g., acoustic or optical phonons, and a certain form of electron-phonon interaction. These phonon spectra are already a product of electron-lattice interactions and their further renormalization by these interactions is unwarranted. In the proper (adiabatic) perturbation theory in the ratio of the electron to ion mass, we start by solving for the energy of the electrons for given ion displacements. We then combine this energy with the Coulomb interaction between the ions to solve the lattice vibrational problem and determine phonon frequencies.

The zeroth-order Hamiltonian for ions has ions interacting via unscreened Coulomb interactions—ionic plasma, where ions oscillate with the plasma frequency. Electrons renormalize these plasma oscillations converting them, for example, into acoustic phonons with no lattice instability along the way. Modern state of the art simulations observe this in "an approximation free way" [23]. Conventional models on the other hand start with an ansatz for the phonon dispersion and electron-phonon interaction. Consider, for example, a model of electrons interacting with acoustic phonons. It is this interaction that renormalizes the phonon spectrum within this model leading to the above lattice instability. However, such a secondary renormalization is double counting as we already renormalized lattice vibrations once to obtain acoustic phonons. Because of this the consensus in the community has been that one should not renormalize the phonons within the Migdal-Eliashberg theory, but instead supplement the theory by experimentally measured phonon frequencies [24,25].

We adopt the same approach in this paper. We keep the phonon spectrum arbitrary and show that the Migdal-Eliashberg theory loses validity at a certain finite λ_c independently of the phonon dispersion law and the momentum dependence of the electron-phonon matrix element, i.e., independently of the underlying electron-phonon Hamiltonian. This is possible because the strong coupling limit of this theory is universal. Similar to its weak coupling limit (BCS theory), there is a single energy scale in this limit [26]. Prior studies mix up the above lattice instability, which is outside of the domain of applicability of the Migdal-Eliashberg theory, with its true breakdown within its domain. Many of them are model-dependent and do not make the necessary distinction between the bare and renormalized electron-phonon coupling constants. Most importantly, they do not eliminate the possibility that the theory remains valid for all λ, including $\lambda = \infty$. It is also important to note that the mechanism of the breakdown we discussed above, while also accompanied by a lattice distortion, is unrelated to the lattice instability due to the artificial phonon softening at $\lambda_0 \approx 0.5$. Indeed, no such softening takes place in our mechanism.

The paper is organized as follows. In Secs. II and III, we review our previous work [14] where we derived the quasiparticle free energy within the Migdal-Eliashberg theory and mapped it to a classical spin chain. We also introduce models we employ in this paper and discuss alternative forms of the Eliashberg equations and the strong coupling limit of the theory. In Sec. IV, we establish that Migdal-Eliashberg theory loses validity for $\lambda > \lambda_c$, where $\lambda_c \lesssim 3.7$. The normal state heat capacity becomes negative for $\lambda > 3.7$ and quasiparticle decay rate is much larger than the temperature. In contrast, the superconducting state is free from such pathologies. We further show in Sec. IV that at strong coupling the low energy part of the quasiparticle spectrum of the superconductor consists of narrow bands of width of the order of the phonon frequency Ω. At high energies, the spectrum is continuous with no gaps. The specific heat is positive at all T in the supeconducting state and the quasiparticle decay rate is negligible. We develop a simple qualitative picture of the breakdown that explains the above pathologies of the normal state in Sec. V. In Sec. VI, we discuss new order that emerges at λ_c and its implications for the electron-phonon system. In Sec. VII, we compare our and previous studies of the Migdal-Eliashberg theory. Section VIII addresses the role of classical phonons in the breakdown and in Sec. IX, we consider the adiabatic limit, $M \to \infty$, that reveals their role especially clearly. In Sec. X, we present our theory of lattice-fermionic superfluidity that remains valid after the Migdal-Eliashberg theory breaks down and accommodates new phases emerging at stronger coupling. In concluding section, we summarize and discuss open questions and some of the implications of our study, such as an upper bound on the superconducting T_c.

II. FREE ENERGY AND ELIASHBERG EQUATIONS

We begin with the description of two electron-phonon models that we use—the Holstein model and a more general model with arbitrary phonon spectrum and momentum dependent electron-phonon interaction. We then review the results of our earlier work where we derived the free energy density functional for the fermionic subsystem for these models. The stationary point equations of this free energy are standard Eliashberg equations, which we also review.

A. Models

We employ two models in this paper. The first one is the Holstein model (dispersionless phonons) with an *arbitrary* hopping matrix and an onsite potential,

$$H = \sum_{ij\sigma} h_{ij} c^\dagger_{i\sigma} c_{j\sigma} + \sum_i \left[\frac{p_i^2}{2M} + \frac{K_0 x_i^2}{2} \right] + \alpha \sum_i n_i x_i, \quad (6)$$

where i and j label the lattice sites, h_{ij} are the matrix elements of an arbitrary single-electron Hamiltonian $\hat{h}$, $c^\dagger_{i\sigma}$ and $c_{i\sigma}$ are creation and annihilation operators for an electron on site i with spin projection σ, $n_i = \sum_\sigma c^\dagger_{i\sigma} c_{i\sigma}$ is the fermion occupation operator, and p_i and x_i are ion momentum and position operators. The *bare* phonon frequency is $\Omega_0 = \sqrt{K_0/M}$.

The second model is a more general Hamiltonian describing electrons interacting with dispersing phonons,

$$\begin{aligned} H = &\sum_{\boldsymbol{p}\sigma} \xi_{\boldsymbol{p}} c^\dagger_{\boldsymbol{p}\sigma} c_{\boldsymbol{p}\sigma} + \sum_{\boldsymbol{q}} \omega_0(\boldsymbol{q}) b^\dagger_{\boldsymbol{q}} b_{\boldsymbol{q}} \\ &+ \frac{1}{\sqrt{N}} \sum_{\boldsymbol{p}\boldsymbol{q}\sigma} \frac{\alpha_{\boldsymbol{q}}}{\sqrt{2M\omega_0(\boldsymbol{q})}} c^\dagger_{\boldsymbol{p}+\boldsymbol{q}\sigma} c_{\boldsymbol{p}\sigma} [b^\dagger_{-\boldsymbol{q}} + b_{\boldsymbol{q}}], \end{aligned} \quad (7)$$

where M is the ion mass and N is the number of lattice sites. The phonon spectrum $\omega_0(\boldsymbol{q})$ and the electron-phonon interaction $\alpha_{\boldsymbol{q}}$ are largely arbitrary, except that we will assume for simplicity that both depend on the magnitude of the momentum only, $\omega_0(\boldsymbol{q}) = \omega_0(q)$ and $\alpha_{\boldsymbol{q}} = \alpha_q$. Both h_{ij} and $\xi_{\boldsymbol{p}}$ contain the chemical potential μ as we include the μN_f term into the Hamiltonians, where N_f is the total fermion number.

B. Free energy functional

In the first paper [14] in our series of four papers [14,18,27] on the Migdal-Eliashberg theory, we derived the free energy functional (effective action) for spatially homogeneous states of the system for both above Hamiltonians. The idea is to integrate out phonons in the path integral and then decouple resulting effective fermion-fermion interaction with three Hubbard-Stratonovich fields Φ, $\Sigma_\uparrow$, and $\Sigma_\downarrow$. Next, we integrate out the fermions, obtain an effective action in terms of the *Eliashberg fields* Φ, $\Sigma_\uparrow$, and $\Sigma_\downarrow$, and look for stationary points where these fields are spatially uniform and depend on the time difference only. We work in the regime where the Fermi energy is the largest energy in the problem, much larger than characteristic interaction and phonon energies. This implies that the single-fermion spectrum is particle-hole symmetric at relevant energies and we also assume time reversal symmetry.

The above steps and setup lead to the following expression for the free energy of the system per site [28],

$$\begin{aligned} f = &\nu_0 T^2 \sum_{nl} [\Phi^*_{n+l} \Lambda_l \Phi_n + \Sigma_{n+l} \Lambda_l \Sigma_n] \\ &- 2\pi \nu_0 T \sum_n \sqrt{(\omega_n + \Sigma_n)^2 + |\Phi_n|^2}. \end{aligned} \quad (8)$$

Here ν_0 is the density of states at the Fermi energy per site per spin projection. The field $\Phi_n \equiv \Phi(i\omega_n)$ is complex and $\Sigma_n \equiv \Sigma(i\omega_n)$ is real. Both fields are functions of the fermionic Matsubara frequency $\omega_n = \pi T(2n+1)$. Particle-hole symmetry implies that $|\Phi_n|$ is even and Σ_n is odd in ω_n. At the stationary point, these fields equal the anomalous and normal self-energies. The effective action is $S_\mathrm{eff} = Nf/T$ with N being the number of lattice sites. At its minimum Eq. (8) gives the grand potential of the system in the thermodynamic limit, but we colloquially refer to it as the free energy. More generally, $e^{-Nf/T}$ determines the weight of a given field configuration in the partition sum.

The quantity Λ_l in Eq. (8) is the Fourier transform of $1/\lambda(\tau)$ at bosonic Matsubara frequency $\omega_l = 2\pi T l$, where $\lambda(\tau)$ is the effective electron-electron interaction in the imaginary time domain. It is more practical to specify $\lambda(\omega_l)$—the Fourier transform of $\lambda(\tau)$ to the Matsubara frequency domain. For the Holstein model, we have

$$\lambda(\omega_l) = \frac{g^2}{\omega_l^2 + \Omega^2}, \quad g^2 = \nu_0 \alpha^2 M^{-1}. \quad (9)$$

For phonons with dispersion,

$$\lambda(\omega_l) = \frac{1}{2p_F^2} \int_0^{2p_F} \frac{g_q^2 q dq}{\omega_l^2 + \omega_q^2}, \quad g_q^2 = \nu_0 |\alpha_q|^2 M^{-1}, \quad (10)$$

where p_F is the Fermi momentum. Here Ω and ω_q are the *renormalized* phonon frequencies, not to be confused with bare frequencies Ω_0 and $\omega_0(q)$. The last expression for $\lambda(\omega_l)$ is for a spherical Fermi surface in $d = 3$ dimensions, but it is straightforward to extend it to any $d \geqslant 2$.

As usual, we define the dimensionless electron-phonon coupling constant as $\lambda = \lambda(\omega_l = 0)$. Then,

$$\begin{aligned} \lambda &= \frac{g^2}{\Omega^2} = \frac{\nu_0 \alpha^2}{K}, \quad \text{Holstein model,} \\ \lambda &= \frac{1}{2p_F^2} \int_0^{2p_F} \frac{g_q^2 q dq}{\omega_q^2}, \quad \text{dispersing phonons,} \end{aligned} \quad (11)$$

where K is the renormalized spring constant. It is also convenient to introduce α, g, K and Ω for dispersing phonons as the following averages:

$$\begin{aligned} \alpha^2 &\equiv \frac{1}{2p_F^2} \int_0^{2p_F} |\alpha_q|^2 q dq, \quad g^2 \equiv \nu_0 \alpha^2 M^{-1}, \\ \Omega^2 &\equiv \frac{g^2}{\lambda}, \quad K \equiv \frac{\nu_0 \alpha^2}{\lambda}. \end{aligned} \quad (12)$$

Often we will consider the strong coupling limit $\lambda \to \infty$, which is equivalent to $\Omega \to 0$ or $K \to 0$.

C. Eliashberg equations

The stationary point equations for the free energy (8) are the well-known *Eliashberg equations* [2],

$$\Phi_n = \pi T \sum_m \lambda_{\rm nm} \frac{\Phi_m}{\sqrt{(\omega_m + \Sigma_m)^2 + |\Phi_m|^2}}, \tag{13a}$$

$$\Sigma_n = \pi T \sum_m \lambda_{\rm nm} \frac{\omega_m + \Sigma_m}{\sqrt{(\omega_m + \Sigma_m)^2 + |\Phi_m|^2}}, \tag{13b}$$

where

$$\lambda_{\rm nm} = \lambda(\omega_n - \omega_m), \quad \lambda_{nn} = \lambda(0) = \lambda. \tag{14}$$

Note that λ_{nn} diverges in the strong coupling limit.

It is convenient to introduce new variables—complex $F(\tau)$ and real $G(\tau)$ defined as

$$\Phi(\tau) = \pi\lambda(\tau)F(\tau), \quad \Sigma(\tau) = \pi\lambda(\tau)G(\tau). \tag{15}$$

In frequency representation, we have

$$\Phi_n = \pi T \sum_m \lambda_{\rm nm} F_m, \quad \Sigma_n = \pi T \sum_m \lambda_{\rm nm} G_m, \tag{16}$$

and Eq. (13) becomes

$$F_n = \frac{\Phi_n}{\sqrt{(\omega_n + \Sigma_n)^2 + |\Phi_n|^2}}, \qquad G_n = \frac{\omega_n + \Sigma_n}{\sqrt{(\omega_n + \Sigma_n)^2 + |\Phi_n|^2}}. \tag{17}$$

On the stationary point, the fields F_n and G_n correspond to the anomalous and normal Green's functions integrated over the single-particle energy [14]. Parity properties of Σ_n and $|\Phi_n|$ imply that G_n is odd and $|F_n|$ is even.

Importantly, it is possible to rewrite the Eliashberg equations (13) so as to eliminate the $m = n$ terms that diverge in the strong coupling limit [14,19]. The new equations have the same form

$$\Phi'_n = \pi T \sum_{m\neq n} \lambda_{\rm nm} \frac{\Phi'_m}{\sqrt{(\omega_m + \Sigma'_m)^2 + |\Phi'_m|^2}}, \tag{18a}$$

$$\Sigma'_n = \pi T \sum_{m\neq n} \lambda_{\rm nm} \frac{\omega_m + \Sigma'_m}{\sqrt{(\omega_m + \Sigma'_m)^2 + |\Phi'_m|^2}}, \tag{18b}$$

where

$$\Phi'_n = \pi T \sum_{m\neq n} \lambda_{\rm nm} F_m, \quad \Sigma'_n = \pi T \sum_{m\neq n} \lambda_{\rm nm} G_m. \tag{19}$$

Troublesome $m = n$ terms are now absent both from the new equations and from the "reduced" self-energies Φ'_n and Σ'_n.

Eliashberg equations generally have more than one solution, e.g., at $T = 0$, there is a solution with $\Phi_n = 0$ and a solution with $\Phi_n \neq 0$. Moreover, we established in Ref. [14] that new "spin flip" solutions emerge at $\lambda \gtrsim 1$. However, most important for us here is the solution with the lowest free energy, which we dub the *Eliashberg stationary point*. This stationary point is the global minimum when the Migdal-Eliashberg theory is a valid description of the system and is a saddle point or a local minimum otherwise.

III. MAPPING TO A SPIN CHAIN

This section concludes the summary of our previous results that we will use to demonstrate the breakdown of the Migdal-Eliashberg theory at strong coupling from within the theory itself. The main result reviewed here is that the free energy functional maps to a classical Heisenberg spin chain. Sites of the chain are fermionic Matsubara frequencies ω_n and the components of classical spin $\boldsymbol{S}_n$ are energy-integrated normal and anomalous Green's functions, $S^z_n = G_n$ and $S^+_n = F_n$, where $S^+_n \equiv S^x_n + iS^y_n$.

Indeed, observe that Eq. (17) implies a constraint on the variables G_n and F_n,

$$G_n^2 + |F_n|^2 = 1. \tag{20}$$

Therefore we can treat these variables as three components of a *classical spin* $\boldsymbol{S}_n$ of unit length, $\boldsymbol{S}_n^2 = 1$,

$$S^z_n = G_n, \quad S^x_n = \mathrm{Re}(F_n), \quad S^y_n = \mathrm{Im}(F_n). \tag{21}$$

It follows from Eq. (17) that

$$F_n\Phi^*_n + G_n(\omega_n + \Sigma_n) = \sqrt{(\omega_n + \Sigma_n)^2 + |\Phi_n|^2}. \tag{22}$$

This allows us to rewrite the free energy density given by Eq. (8) as

$$f = \nu_0 T H_s, \text{ where} \tag{23}$$

$$H_s = -2\pi \sum_n \omega_n S^z_n - \pi^2 T \sum_{\rm nm} \lambda_{\rm nm}(\boldsymbol{S}_n \cdot \boldsymbol{S}_m - 1). \tag{24}$$

We interpret H_s as a Hamiltonian of an open classical Heisenberg spin chain in an inhomogeneous "Zeeman magnetic field." The positions of the spins are fermionic Matsubara frequencies ω_n. Spin-spin interactions are ferromagnetic and fall off at large "distance" as $\lambda_{\rm nm} \propto (\omega_n - \omega_m)^{-2}$. The magnetic field is linear in the position of the spin and goes to $\pm\infty$ as $\omega_n \to \pm\infty$. Eliashberg equations (13) are spin equilibria conditions that enforce parallel alignment of each spin and the effective magnetic field acting on it (Zeeman field plus the field from other spins).

In particular, for the Holstein model substituting Eq. (9) into Eq. (24), we obtain

$$H_s = -2\pi \sum_n \omega_n S^z_n - \pi^2 T g^2 \sum_{\rm nm} \frac{\boldsymbol{S}_n \cdot \boldsymbol{S}_m - 1}{(\omega_n - \omega_m)^2 + \Omega^2}. \tag{25}$$

In general, the spin chain representations (24) and (25) of the free energy are guaranteed to work only at its stationary points, because we used Eqs. (20) and (22) that derive from the stationary point equations to obtain them. It is also important to keep in mind that f is the contribution of the fermionic degrees of freedom (quasiparticles) to the free energy. The total free energy is f plus the free energy (grand potential) of noninteracting phonons. See Ref. [14] for a comprehensive discussion of properties and consequences of the spin chain representation of the free energy.

Now let us develop a minidictionary between the original language of superconductivity and the spin terminology. First of all, similar to the Anderson pseudospin description of the BCS theory of superconductivity [29], the superconducting transition translates into softening of the domain wall as shown in Fig. 2. This is a result of the competition between

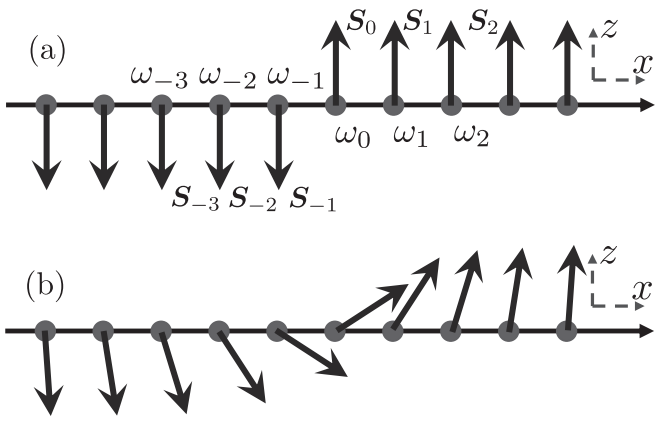

FIG. 2. Classical spin representation of the transition from (a) the normal to (b) superconducting state. As discussed in the text, the Migdal-Eliashberg theory maps to a classical Heisenberg spin chain. The positions of the spins are fermionic Matsubara frequencies ω_n. Spin-spin interactions are purely ferromagnetic and the spins are subject to a Zeeman magnetic field $2\pi\omega_n$ along the z axis. In the superconducting state, spins acquire x components, which implies nonzero anomalous Green's function. The sharp domain wall in the normal state is smeared in the superconducting state.

the Zeeman magnetic field and ferromagnetic interaction in H_s. The spin configuration minimizing the Zeeman term is $\boldsymbol{S}_n = \mathrm{sgn}(\omega_n)\hat{\boldsymbol{z}}$, and the Zeeman field necessarily prevails at large $|\omega_n|$, so that $\boldsymbol{S}_n \to \pm\hat{\boldsymbol{z}}$ for $\omega_n \to \pm\infty$.

Above the superconducting T_c, the anomalous averages vanish, $F_n = 0$. According to the definition (21) of the classical spin, this implies that all spins are parallel to the z axis. From the behavior of $\boldsymbol{S}_n$ at large ω_n and by symmetry, it is then clear that the minimum energy spin texture is

$$\boldsymbol{S}_n = \mathrm{sgn}(\omega_n)\hat{\boldsymbol{z}}. \tag{26}$$

This is the *normal state* in the spin language. Its characteristic feature is a sharp domain wall between ω_{-1} and ω_0 with an abrupt jump of the z component of spin from $S^z_{-1} = -1$ to $S^z_0 = +1$, see Fig. 2.

Below T_c, the anomalous averages are nonzero, i.e., the spins acquire x-components (F_n can be made real in the spin chain ground state). In other words, the domain wall softens in superconducting states. Now the change in S^z_n from -1 at $\omega_n = -\infty$ to $+1$ at $\omega_n = +\infty$ occurs gradually and the jump $S^z_0 - S^z_{-1} < 2$.

A. Strong coupling limit

We will see in the next section that the Migdal-Eliashberg theory stops being a valid description of any physical system for values of the renormalized electron-phonon coupling $\lambda \geqslant \lambda_c$, where $\lambda_c \lesssim \lambda_* \approx 3.69$. One may ask then, what is the point in considering its strong coupling, $\lambda \to \infty$, limit where the theory is unphysical. The main point is that the answers for any observable obtained with different underlying electron-phonon models, i.e., for different phonon spectra and electron-phonon matrix elements, converge in this limit—the strong coupling limit of the Migdal-Eliashberg theory is universal, see, e.g., Ref. [26].

For example, suppose we evaluated the specific heat for the Holstein model, $c_H(T, \lambda)$, as a function of temperature and λ. At $\lambda = \infty$ the specific heat, $c_g(T, \lambda)$, for a general electron-phonon model (7) coincides with $c_H(T, \lambda)$, $c_g(T, \infty) = c_H(T, \infty)$. At large but finite λ, $c_g(T, \lambda)$ is close to $c_H(T, \lambda)$ and we can make them arbitrarily close by increasing λ. In particular, we will see that the value $\lambda_* \approx 3.69$ obtains from the condition $\min[c_H(T, \lambda_*)] = 0$ for $T > T_c$. The universality of the strong coupling limit implies that there is finite λ_c for the general electron-phonon model as well. Moreover, since $\lambda_* \approx 3.69$ is already quite large, the values of λ_* obtained for different models should be close to 3.69.

The strong coupling limit is equivalent [14,26] to sending all (renormalized) phonon frequencies to zero, $\omega_q \to 0$ and $\Omega \to 0$. Then the effective electron-electron interaction (10) becomes

$$\lambda(\omega_l) = \frac{g^2}{\omega_l^2}, \tag{27}$$

where for the Holstein model $g^2 = \nu_0\alpha^2 M^{-1}$ as before, while for the dispersing phonon model (7) the constant g^2 is given by Eq. (12). The free energy functional (8) becomes in this limit [14]

$$H_s = -2\pi \sum_n \omega_n S^z_n - \pi^2 T g^2 \sum_{\mathrm{nm}} \frac{\boldsymbol{S}_n \cdot \boldsymbol{S}_m - 1}{(\omega_n - \omega_m)^2}. \tag{28}$$

We see explicitly that H_s is independent of the underlying microscopic model except through a single constant g. Moreover, the $\lambda \to \infty$ limit has another convenient property—in this case the expression (28) for the free energy holds at all points (G_n, F_n) of the configuration space, unlike finite λ, for which the spin chain representation (24) applies only at the stationary points of Eq. (8), see Ref. [14] for more detail.

IV. BREAKDOWN OF THE MIGDAL-ELIASHBERG THEORY

We present indisputable evidence of the breakdown of the Migdal-Eliashberg theory at strong coupling. The critical value of the renormalized electron-phonon coupling λ_c above which the theory becomes unphysical lies in the interval $3.0 \lesssim \lambda_c \lesssim 3.7$. We provide two pieces of such evidence. First, the normal state specific heat evaluated within this theory becomes negative above T_c for $\lambda \geqslant 3.7$ indicating that this state is thermodynamically unstable [4].

Second, quasiparticle lifetime vanishes in the normal state as $\tau = [\mathrm{Im}\Sigma(\omega)]^{-1} \approx (\pi\lambda T)^{-1} \to 0$ when $\lambda \to \infty$ signaling a complete breakdown of the quasiparticle picture. It indicates that the Migdal-Eliashberg theory no longer employs the correct zeroth-order (in electron-phonon coupling) Hamiltonian for fermions. The true normal state cannot be a Fermi liquid with the translational symmetry of the lattice anymore. We will see that this short lifetime is entirely due to the thermal fluctuations of static displacements of the ions from their equilibrium positions, see also Ref. [19].

On the other hand, the behavior of these quantities in the superconducting state at strong coupling is diametrically opposite. The specific heat is positive for all $T \leqslant T_c$ and exhibits activated behavior at low temperatures. Quasiparticle lifetime is exponentially large at $\lambda = \infty$ and proportional to

$\sqrt{\lambda}$ at large but finite λ. However, this does not mean that the superconducting state predicted by this theory is "out of the woods" and indeed we will see in the next section that, at least for a range of temperatures below T_c, it is not the true thermal equilibrium of the electron-phonon system.

By construction solutions of the Eliashberg equations (13) are stationary points of the free energy functional for any coupling λ. The above findings demonstrate that for $\lambda > \lambda_c$ none of these stationary points is the true global minimum of the free energy, at least in a certain temperature range that includes temperatures both above and below T_c. In subsequent sections, we will see that this happens due to a phase transition that breaks the translational invariance of the lattice. This transition is independent of the lattice instability discussed in Introduction and does not rely on conventional electron-phonon models for its existence.

A. Normal state specific heat

We start by rederiving the specific heat for the Holstein model within the Migdal-Eliashberg theory [30] with the help of the spin chain Hamiltonian,

$$H_s = -2\pi \sum_n \omega_n S_n^z - \pi^2 T g^2 \sum_{\rm nm} \frac{\boldsymbol{S}_n \cdot \boldsymbol{S}_m - 1}{(\omega_n - \omega_m)^2 + \Omega^2}. \quad (29)$$

By definition (23) of the spin Hamiltonian, the free energy is $f = \nu_0 T H_s$. We saw in Sec. III that in the normal state,

$$S_n^z = \mathrm{sgn}(\omega_n), \quad S_n^x = S_n^y = 0. \quad (30)$$

Therefore the normal state free energy is

$$f_{\rm n} = -2\pi \nu_0 T \sum_n \omega_n \mathrm{sgn}(\omega_n) - \pi^2 \nu_0 T^2 g^2 \sum_{\rm nm} \frac{\mathrm{sgn}(\omega_n \omega_m) - 1}{(\omega_n - \omega_m)^2 + \Omega^2}. \quad (31)$$

The first term on the right is the temperature-dependent part of the free energy of noninteracting electrons [31],

$$f_0 = -\frac{\pi^2 \nu_0 T^2}{3}. \quad (32)$$

Note that $\mathrm{sgn}(\omega_n \omega_m) - 1$ vanishes when ω_n and ω_m have the same sign and is equal to -2 otherwise. This observation allows us to rewrite the second term (interaction part of the free energy) as

$$f_{\rm int} = \nu_0 g^2 \sum_{l=1}^{\infty} \frac{l}{l^2 + a^2}, \quad a \equiv \frac{\Omega}{2\pi T}. \quad (33)$$

We also reduced the summation over n and m to a single sum over $l = n + m + 1$ using $\omega_n - (-\omega_m) \propto (n + m + 1)$ and taking into account that there are l ways to choose n and m for a given value of l.

The sum in Eq. (33) is logarithmically divergent [33]. Nonetheless, let us write the summand as a sum of two simple fractions and use the following property of the digamma function $\psi(x)$:

$$\sum_{l=1}^{\infty} \left(\frac{1}{x + l} - \frac{1}{l} \right) = -\frac{1}{x} - \psi(x) - \gamma, \quad (34)$$

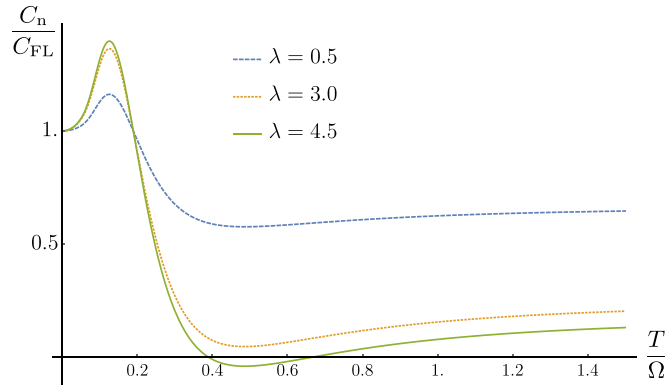

FIG. 3. Normal state quasiparticle specific heat $C_{\rm n}$ in the Migdal-Eliashberg theory as a function of the ratio T/Ω of the temperature to Einstein phonon frequency for three different values of electron-phonon coupling λ. We normalize $C_{\rm n}$ by its low-temperature Fermi liquid asymptote $C_{\rm FL} = \gamma_0 T(1 + \lambda)$. Note that for $\lambda = 4.5$, the specific heat is *negative* above the superconducting $T_c \approx 0.4\Omega$ signaling the *breakdown* of the Migdal-Eliashberg theory at strong coupling. Since the $\lambda \to \infty$ limit of this theory is universal, it breaks down irrespective of the underlying electron-phonon model.

where γ is Euler's constant. We find

$$\sum_{l=1}^{\infty} \frac{l}{l^2 + a^2} = \mathrm{Re}[\psi(ia)] + \sum_{l=1}^{l_0} \frac{1}{l} - \gamma, \quad (35)$$

where we truncated the sum on the right-hand side at l_0. For large l_0, the last two terms sum to $\ln l_0$ with an error of order $1/l_0$. Since $\Lambda = 2\pi T l_0$ is a Matsubara frequency, it is safe to replace these two terms with $\ln \frac{\Lambda}{2\pi T}$, where Λ is the frequency cutoff.

Note that Λ affects only the temperature-independent part of the free energy that we are not attempting to evaluate anyway. This part is the ground state energy per site; it diverges because we sent the Fermi energy to infinity when deriving the free energy. Thus the temperature-dependence of the free energy density in the normal state is

$$f_{\rm n} = -\frac{\pi^2 \nu_0 T^2}{3} - \nu_0 g^2 \mathrm{Re}[\psi(ia)] - \nu_0 g^2 \ln T. \quad (36)$$

The corresponding specific heat (heat capacity per site) is

$$C_{\rm n} = -T \frac{d^2 f}{dT^2} = \gamma_0 T \left[1 + \lambda h\left(\frac{\Omega}{2\pi T} \right) \right], \quad (37)$$

where

$$\gamma_0 = \frac{2\pi^2 \nu_0}{3} \quad (38)$$

is the specific heat coefficient of free electrons, $\lambda = \frac{g^2}{\Omega^2}$, and

$$h(x) = -6x^2 - 12x^3 \mathrm{Im}[\psi'(ix)] - 6x^4 \mathrm{Re}[\psi''(ix)]. \quad (39)$$

The same expression (37) obtains by a different method [30], which provides an independent check on the spin chain representation of the free energy.

We show three representative plots of $C_{\rm n}(T)$ in Fig. 3. Notice that, for instance, for $\lambda = 4.5$ the specific heat is negative in an interval of temperatures from $T_- \approx 0.4\Omega$ to $T_+ \approx 0.7\Omega$.

The superconducting transition temperature for large λ is $T_c \approx 0.18\sqrt{\lambda}\Omega$ [20], which for $\lambda = 4.5$ is $T_c \approx 0.4\Omega$. Hence the quasiparticle heat capacity is negative above T_c.

Let us determine the value of λ at which the specific heat becomes negative for the first time. The function $h(x)$ in Eq. (37) has a single minimum $h_{\min} = -0.2709$ at $x_{\min} = 0.3273$. The normal state specific heat $C_{\rm n}$ becomes negative for $\lambda > -h_{\min}^{-1} \equiv \lambda_* \approx 3.69$. The normal-superconductor transition for $\lambda = \lambda_*$ occurs at $T_c \approx 0.35\Omega$. The minimum of the function $\frac{C_{\rm n}(T)}{C_{\rm FL}}$, where $C_{\rm FL} = \gamma_0 T(1+\lambda)$ is at $T_{\min} = (2\pi x_{\min})^{-1}\Omega \approx 0.49\Omega$. At this temperature the specific heat is always negative for $\lambda > \lambda_*$.

Therefore, for any $\lambda > \lambda_*$, the quasiparticle specific heat is negative in an interval of temperatures (T_-, T_+), where $T_+ > T_c$,

$$C_{\rm n}(T) < 0 \text{ for } \lambda > \lambda_* \approx 3.69 \text{ and } T_- < T < T_+. \tag{40}$$

The length of this interval starts from zero at $\lambda = \lambda^*$ and grows monotonically with λ. At first, both T_+ and T_- are above T_c until T_- falls below it. At large λ,

$$T_- \approx 0.31\Omega, \quad T_+ \approx 0.38\sqrt{\lambda}\Omega, \tag{41}$$

where we took the large λ asymptote of T_+ from Eq. (43) below and for T_- we obtained it from $h(x_0) = 0$. The numerical solution is $x_0 \approx 0.5100$ and therefore $T_- = (2\pi x_0)^{-1}\Omega \approx 0.31\Omega$ for $\lambda \to \infty$.

In the strong coupling limit $\lambda \to \infty$ and $\Omega \to 0$, so that $g^2 = \lambda\Omega^2 =$ fixed. Then, $T \gg \Omega$ and with the help of the series expansion for the digamma function, we find that Eq. (37) becomes

$$C_{\rm n} = \gamma_0 T\left[1 - \left(\frac{T_+}{T}\right)^2\right], \tag{42}$$

$$T_+ = g\sqrt{\frac{3}{2\pi^2}} \approx 0.38g. \tag{43}$$

This is negative for all temperatures below T_+ and again $T_+ > T_c$.

It is also instructive to evaluate $C_{\rm n}$ in the strong coupling limit directly from Eq. (33), where now $a = 0$. We have

$$\frac{f_{\rm int}}{\nu_0 g^2} = \sum_{l=1}^{l_0} \frac{1}{l} = \int_{2\pi T}^{\Lambda} \frac{d\omega_l}{\omega_l} + \gamma. \tag{44}$$

Here we introduced a cutoff as discussed below Eq. (35). Combining this with f_0 in Eq. (32), we obtain

$$f_{\rm n} = -\frac{\pi^2 \nu_0 T^2}{3} - \nu_0 g^2 \ln T. \tag{45}$$

The normal state entropy $S_{\rm n}$ and specific heat $C_{\rm n}$ therefore are

$$S_{\rm n} = -\frac{df}{dT} = \gamma_0 T + \frac{\nu_0 g^2}{T}, \tag{46}$$

$$C_{\rm n} = -T\frac{d^2 f}{dT^2} = \gamma_0 T - \frac{\nu_0 g^2}{T}. \tag{47}$$

This $C_{\rm n}$ coincides with Eq. (42).

Recall that f is the contribution of the fermionic quasiparticles to the total free energy, which is f plus the free energy of noninteracting thermal phonons. The combined specific heat of quasiparticles and phonons is positive. For example, the specific heat of Einstein phonons in 3D at $T \gg \Omega$ is $C_E = 3n_i$. Assuming the number density of ions n_i is the same as that of electrons, $C_E = 2\nu_0\varepsilon_F$. This is much larger in magnitude than the minimum $C_{\rm n} \sim -\nu_0 g$ above T_c [see Eq. (42)], since $\varepsilon_F \gg g$. However, looking back at the derivation of the Eliashberg free energy in Ref. [14], we observe that the partition function of the system is of the from $\mathcal{Z} = \mathcal{Z}_s\mathcal{Z}_p$. Here $\mathcal{Z}_s$ is the partition function of our classical spin chain or, equivalently, of the fermionic degrees of freedom and $\mathcal{Z}_p$ is the partition function of noninteracting phonons. Thus phonons and quasiparticles are two decoupled subsystems in the Migdal-Eliashberg theory as true quasiparticles must be. Both subsystems should have positive heat capacities or the system is thermodynamically unstable [4].

We conclude that the quasiparticle picture breaks down for large electron-phonon coupling λ together with the Migdal-Eliashberg theory based on it. This result is independent of the model electron-phonon Hamiltonian, since at strong coupling the free energy functional always converges to the spin chain Hamiltonian (29) as discussed in Sec. III A. The critical value of λ where the Eliashberg stationary point ceases to be the global minimum must be in any case no larger than λ_* at which the quasiparticle specific heat turns negative. We expect the precise values of λ_c and λ_* to dependent only weakly on the underlying model, because $\lambda_* \approx 3.69$, we obtained for the Holstein model is already quite deep in the strong coupling regime where all models converge. There are reportedly [34] materials ($Pb_{0.5}Bi_{0.5}$) with $\lambda \approx 3.0$ that are well described by the Migdal-Eliashberg theory. Therefore we expect

$$3.0 \leqslant \lambda_c \leqslant 3.7. \tag{48}$$

B. Specific heat and entropy in the superconducting state

In stark contrast to the normal state, thermodynamics of the superconducting state is free of pathologies. The specific heat is positive at any coupling strength and the entropy vanishes when $T \to 0$ as it should. To show this, it is sufficient to analyze the worst case scenario $\lambda = \infty$. In this limit, we are able to determine thermodynamic properties at low temperatures and temperatures just below T_c essentially analytically, while computing them for general λ would require substantial numerical work. Since the strong coupling limit of the Migdal-Eliashberg theory is model-independent, our results apply equally well to the Holstein Hamiltonian (6) and the general electron-phonon model (7).

Consider temperatures near T_c. The jump in the specific heat at T_c for $\lambda = \infty$ is [34]

$$\Delta C = C_{\rm sc} - C_{\rm n} \approx 19.9\,\gamma_0 T_c. \tag{49}$$

Setting $T_c \approx 0.18g$ in Eq. (47), we determine the normal state specific heat at $T = T_c$,

$$C_{\rm n}(T_c) \approx -3.7\gamma_0 T_c. \tag{50}$$

Therefore the specific heat in the superconducting state at $T = T_c$ is

$$C_{\rm sc}(T_c) \approx 16.2\,\gamma_0 T_c. \tag{51}$$

We see that the specific heat is positive just below T_c.

Now let as evaluate the entropy and specific heat at low temperatures. At the global minimum, the spins $\boldsymbol{S}_n$ are

coplanar [14]. Choosing the x axis so that $S_n^y = 0$, we have

$$S_n^z = \cos\theta_n, \quad S_n^x = \sin\theta_n, \tag{52}$$

where θ_n is the angle the spin makes with the z axis. Expressing the spin chain Hamiltonian (29) in terms of θ_n, we obtain the free energy in the form

$$f_{\rm sc} = -2\pi\nu_0 T\sum_n \omega_n\cos\theta_n - \pi^2\nu_0 T^2 g^2\sum_{\rm nm}\frac{\cos(\theta_n-\theta_m)-1}{(\omega_n-\omega_m)^2+\Omega^2}. \tag{53}$$

The stationary point equation, $\partial f_{\rm sc}/\partial\theta_n = 0$, for $f_{\rm sc}$ is

$$\omega_n\sin\theta_n = \pi T g^2\sum_m\frac{\sin(\theta_m-\theta_n)}{(\omega_n-\omega_m)^2+\Omega^2}. \tag{54}$$

This is nothing but the Eliashberg gap equation written in terms of θ_n [14].

The relationship between the gap function $\Delta(i\omega_n)\equiv\Delta_n$ and θ_n is

$$\cos\theta_n = \frac{\omega_n}{\sqrt{\omega_n^2+\Delta_n^2}}, \quad \sin\theta_n = \frac{\Delta_n}{\sqrt{\omega_n^2+\Delta_n^2}}. \tag{55}$$

The gap equation also follows from Eq. (13a) after we substitute

$$\Phi_n = \Delta_n Z_n, \quad \omega_n+\Sigma_n = \omega_n Z_n, \tag{56}$$

and express Z_n in terms of Δ_n from Eq. (13b). Eliashberg equations (13) become

$$\omega_n\Delta_n = \pi T\sum_m\lambda_{\rm nm}\frac{\omega_n\Delta_m-\Delta_n\omega_m}{\sqrt{\omega_m^2+|\Delta_m|^2}}, \tag{57a}$$

$$Z_n = 1+\frac{\pi T}{\omega_n}\sum_m\lambda_{\rm nm}\frac{\omega_m}{\sqrt{\omega_m^2+|\Delta_m|^2}}. \tag{57b}$$

The replacement (55) turns Eq. (57a) into Eq. (54).

It is helpful to introduce the *condensation energy*,

$$\delta f = f_{\rm sc}-f_{\rm n} = -2\pi\nu_0 T\sum_n(\omega_n\cos\theta_n-|\omega_n|) - \frac{\nu_0 g^2}{4}\sum_{n\neq m}\frac{\cos(\theta_n-\theta_m)-{\rm sgn}(\omega_n\omega_m)}{(n-m)^2}, \tag{58}$$

where we took the strong coupling limit $\Omega\to 0$ and used $\omega_n = \pi T(2n+1)$. A helpful property of this expression is that all sums in it converge as long as $\sum_{n>0} n\theta_n^2 < \infty$ [35] unlike in Eqs. (31) and (53). This is important because, for example, it is due to the divergence of the double sum in Eq. (31) that we gained the $\ln T$ term in Eq. (45). Had this sum converged, it would contribute only a temperature independent constant with no effect on the entropy and specific heat. Since $\Delta_n\to 0$ as $n\to\infty$, Eq. (55) implies $\theta_n = o(n^{-1})$ and therefore $\sum_{n>0} n\theta_n^2 < \infty$.

In the strong coupling limit, differentiation of the condensation energy with respect to T simplifies considerably, since the interaction term in Eq. (58) has no explicit temperature dependence—its only dependence on T is through θ_n. We need δf at the stationary points and because at these points $\partial[\delta f]/\partial\theta_n = 0$, we have

$$\frac{d[\delta f]}{dT} = \frac{\partial[\delta f]}{\partial T}+\sum_n\frac{\partial[\delta f]}{\partial\theta_n}\frac{\partial\theta_n}{\partial T} = \frac{\partial[\delta f]}{\partial T}. \tag{59}$$

Applying this formula to Eq. (58), we find

$$\frac{d[\delta f]}{dT} = -8\pi\nu_0\sum_{n=0}^{\infty}\left(\frac{\omega_n^2}{\sqrt{\omega_n^2+\Delta_n^2}}-\omega_n\right), \tag{60}$$

where Δ_n is the solution of the gap equation (54). We calculate this Matsubara sum in Appendix A. Notably, we obtain an interesting identity along the way,

$$\int_0^\infty d\omega\left(\omega-\frac{\omega^2}{\sqrt{\omega^2+\Delta^2(i\omega)}}\right) = \frac{g^2}{4}. \tag{61}$$

Here $\Delta(i\omega)$ is the Eliashberg gap function on the Matsubara axis at zero temperature in the strong coupling limit.

The end result for the entropy $S_{\rm sc}$ and specific heat $C_{\rm sc}$ in the superconducting state at low T and $\lambda=\infty$ is (see Appendix A)

$$S_{\rm sc}\approx 17.84\nu_0\frac{E_1}{T}e^{-E_1/T}, \quad E_1\approx 1.16g, \tag{62}$$

$$C_{\rm sc}\approx 17.84\nu_0\left(\frac{E_1}{T}\right)^2 e^{-E_1/T}. \tag{63}$$

The specific heat is positive and the entropy vanishes when $T\to 0$ as it should.

Therefore there are no apparent pathologies in the thermodynamics of the Migdal-Eliashberg superconducting state. Of course, this does not prove this state is necessarily the global minimum of the free energy below T_c and we will later see that in fact it is not at least in some range of temperatures.

C. Quasiparticle lifetime: normal state

It is natural to confirm the breakdown of the quasiparticle picture by analyzing quasiparticle lifetimes at large λ. Consider the normal and anomalous thermal Green's functions defined as

$$\mathcal{G}_{\boldsymbol{p}}(\tau-\tau') = -\langle T_\tau c_{\boldsymbol{p}\sigma}(\tau)c^\dagger_{\boldsymbol{p}\sigma}(\tau')\rangle, \tag{64}$$

$$\mathcal{F}_{\boldsymbol{p}}(\tau-\tau') = \langle T_\tau c_{-\boldsymbol{p}\downarrow}(\tau)c_{\boldsymbol{p}\uparrow}(\tau')\rangle. \tag{65}$$

In the Migdal-Eliashberg theory, these Green's functions are in the Matsubara frequency domain, see, e.g., Ref. [14],

$$\mathcal{G}_{\boldsymbol{p}n} = -\frac{i(\omega_n+\Sigma_n)+\xi_{\boldsymbol{p}}}{(\omega_n+\Sigma_n)^2+|\Phi_n|^2+\xi_{\boldsymbol{p}}^2}, \tag{66}$$

$$\mathcal{F}_{\boldsymbol{p}n} = -\frac{\Phi_n}{(\omega_n+\Sigma_n)^2+|\Phi_n|^2+\xi_{\boldsymbol{p}}^2}. \tag{67}$$

In the normal state, $\Phi_n = 0$ and therefore,

$$\mathcal{G}_{\boldsymbol{p}}(\omega_n) = \frac{1}{i\omega_n+i\Sigma_n-\xi_{\boldsymbol{p}}}. \tag{68}$$

Further, Eqs. (16), (21), and (30) imply

$$\Sigma_n = \pi T\sum_m\lambda_{\rm nm}{\rm sgn}(\omega_n). \tag{69}$$

Since in the strong coupling regime the characteristic phonon frequency $\Omega\to 0$, we take T to be much greater than Ω. Then,

the $n = m$ term dominates the summation and we obtain $\Sigma_n = \lambda\pi T\,\mathrm{sgn}(\omega_n)$ and therefore,

$$\mathcal{G}_{\boldsymbol{p}}(\omega_n) = \frac{1}{i\omega_n - \xi_{\boldsymbol{p}} + i\lambda\pi T\,\mathrm{sgn}(\omega_n)}. \tag{70}$$

It is straightforward to analytically continue this to the upper half-plane of complex ω [36] to get the retarded Green's function,

$$G^R_{\boldsymbol{p}}(\omega) = \frac{1}{\omega - \xi_{\boldsymbol{p}} + i\lambda\pi T}. \tag{71}$$

Observe that the quasiparticle decay rate in the normal state,

$$\Gamma_{\mathrm{n}} = \tau_{\mathrm{n}}^{-1} = \lambda\pi T, \tag{72}$$

is much larger than the temperature. The lifetime τ tends to zero as $\lambda \to \infty$. This means that the fermionic quasiparticles are ill-defined in agreement with our specific heat argument.

D. Quasiparticle spectrum in the superconducting state

Before we estimate quasiparticle lifetimes in the superconducting state at large λ, we need to know the properties of the excitation spectrum in this regime. We will see that the low energy part of the quasiparticle spectrum consists of narrow bands of width $g\lambda^{-1/2}$. The gaps between the bands decrease with energy E as E^{-1} until the spectrum becomes continuous above $E_{ct} \sim g\lambda^{1/2}$, when the bandwidth is comparable to the gaps. This is consistent with the expectation of Fermi-liquid-like spectrum at energies of the order of ε_F. Indeed, Migdal's theorem [1] requires

$$x_M = \frac{\lambda\Omega}{\varepsilon_F} \ll 1. \tag{73}$$

Since $\lambda = g^2/\Omega^2$, this implies $\varepsilon_F \gg E_{ct}$.

To determine the spectrum, we first obtain the leading large λ asymptotic behavior of Z_n from Eq. (57b),

$$Z_n = \lambda\pi T\left(\omega_n^2 + \Delta_n^2\right)^{-1/2}. \tag{74}$$

Since Δ_n remains finite the limit $\lambda \to \infty$ [26,37], Z_n diverges at any finite ω_n. Assuming $\xi_{\boldsymbol{p}}$ is also finite and performing the variable change (56) in Eq. (66), we find

$$\mathcal{G}_{pn} = \frac{-i\omega_n}{\lambda\pi T\sqrt{\Delta_n^2 + \omega_n^2}}, \tag{75}$$

where we substituted Z_n from Eq. (74). Analytic continuation to the upper half plane [36] gives

$$G^R_{\boldsymbol{p}}(\omega) = \frac{-\omega}{\lambda\pi T\sqrt{\Delta^2(\omega) - \omega^2}}. \tag{76}$$

Recall the Lehmann representation for the retarded Green's function [38]:

$$G^R_{\boldsymbol{p}}(\omega) = \sum_k \frac{|\langle k|c_{\boldsymbol{p}}|0\rangle|^2}{\omega - E_k + i0^+} + \sum_k \frac{|\langle 0|c_{\boldsymbol{p}}|k\rangle|^2}{\omega + E_k + i0^+}. \tag{77}$$

Here $|k\rangle$ are the eigenstates of the electron-phonon Hamiltonian, E_k are single electron excitation energies (energy differences between eigenstates with $N_{\mathrm{e}} \pm 1$ electrons and the ground state with N_{e} electrons), and we set $T = 0$.

Comparing Eqs. (76) and (77), we conclude that

$$\frac{\omega}{\sqrt{\Delta^2(\omega) - \omega^2}} = \sum_k \left(\frac{P_k}{\omega - E_k} + \frac{P_k}{\omega + E_k}\right), \tag{78}$$

where we absorbed $i0^+$ into ω and

$$P_k = \pi \lim_{T\to 0}\lim_{\lambda\to\infty} (\lambda T|\langle k|c_{\boldsymbol{p}}|0\rangle|^2). \tag{79}$$

P_k must be finite and well-defined, because $\Delta(\omega)$ is finite and well-defined in this limit. Residues at $\omega = \pm E_k$ are equal by particle-hole symmetry [see the discussion above Eq. (8)]. The limits $\lambda \to \infty$ and $T \to 0$ commute for the gap function—one obtains the same $\Delta(\omega)$ no matter in which order these limits are taken [26]. However, they do not commute in general. For example, we saw in the previous paper [14] that there are solutions of the Eliashberg equations that are present for one order of limits and absent for the other. We always take the limit $\lambda \to \infty$ first. Note also that the density of quasiparticle states at any λ is

$$\frac{\nu(\omega)}{\nu_0} = \mathrm{Im}\left[\frac{\omega}{\sqrt{\Delta^2(\omega) - \omega^2}}\right], \tag{80}$$

which we derive by integrating Eq. (66) over $\xi_{\boldsymbol{p}}$.

Equation (78) has several remarkable consequences. Consider real values of ω. First, because the right-hand side is real, $\Delta(\omega)$ must also be real except for a discrete set of points (zeros of the right-hand side) where $\mathrm{Im}\,\Delta(\omega)$ must be infinite. In other words, $\mathrm{Im}\,\Delta(\omega)$ is a sum of delta functions. Moreover, $|\Delta(\omega)| \geqslant |\omega|$ for the same reason. Second, excitation energies $\pm E_k$ are solutions of the equation

$$\Delta(\omega) = \pm\omega. \tag{81}$$

The roots of this equation are necessarily doubly degenerate, since the right-hand side of Eq. (78) has poles rather than branching points at these values of ω. This also follows from $|\Delta(\omega)| \geqslant |\omega|$ as this inequality implies that at $\omega = \pm E_k$ one of the lines $\pm\omega$ is tangent to $\Delta(\omega)$.

Most important for our purpose is the observation that solutions of Eq. (81) form a discrete set and therefore the low energy quasiparticle spectrum is discrete. Indeed, two analytic functions cannot coincide on an interval without being identically equal. Since Eq. (81) does not hold for all ω, it can hold only at a discrete set of points $\pm E_k$, where $k = 1, 2, \ldots$ These corollaries of Eq. (78) reproduce and confirm the results of a more thorough study of the quasiparticle spectrum in the strong coupling limit by Combescot [26]. Since g is the only energy scale left in this limit, E_k/g are numbers of order one. In particular, Combescot finds $E_1 = 1.16g$ and $E_2 = 3.04g$, while for large k,

$$E_k = \pi g\sqrt{k}. \tag{82}$$

Levels E_k are macroscopically degenerate with the degree of the degeneracy controlled by the residue P_k in Eq. (78). It is interesting to note here that the excitation spectrum of the BCS model in the strong coupling limit is a discrete set of macroscopically degenerate levels as well [39].

At finite λ, levels E_k split into energy bands. We show in Appendix B that the width of these bands is approximately $\Omega = g\lambda^{-1/2}$. It follows from Eq. (82) that the gaps between

bands decrease as $\frac{\pi g}{2\sqrt{k}}$ with the band number k. The spectrum becomes continuous when the bandwidth becomes equal to the gap, i.e., for

$$E \geqslant E_{ct} = \frac{\pi^2 g\sqrt{\lambda}}{2}. \tag{83}$$

And indeed we expect continuous spectrum at energies of the order of the Fermi energy, much larger than typical energies associated with superconductivity. At such energies the system must be a Fermi liquid. For sufficiently large ω_n, $|\Phi_n| = Z_n\Delta_n$ is much smaller than $\omega_n + \Sigma_n = Z_n\omega_n$ in the normal Green's function $\mathcal{G}_{pn}$ given by Eq. (66). Neglecting $|\Phi_n|$, we obtain the normal state Green's function (71) and recover Fermi liquid dispersion ξ_p. One has to be careful here because, while Δ_n is of order g at large λ and quickly decreases for $\omega_n > g$, the gap function $\Delta(\omega)$ along the real frequency axis does not necessarily behave in the same way. Along the real axis $\Delta(\omega)$ should in fact decrease substantially only at energies where the spectrum becomes continuous, i.e., at an energy scale $E_{ct} \gg g$. Nevertheless, the smallness of the Migdal's parameter x_M guarantees that the Fermi energy is even larger as seen from Eq. (73).

E. Quasiparticle lifetime: superconducting state

As with thermodynamic properties, the situation with quasiparticle decay predicted by the Migdal-Eliashberg theory for the superconducting state at strong coupling is in some sense opposite to that in the normal state. Consider $\lambda = \infty$ first. Equation (78) shows that the density of states at $T = 0$ is a sum of delta functions. The width of quasiparticle peaks at E_k is zero and the lifetime is therefore infinite. At $T \neq 0$, thermally activated transitions between quasiparticle energy levels E_k occur. However, their rate is exponentially small at low temperature. Direct transitions with an absorption or emission of a phonon are prohibited because the phonon energy $\Omega/g \to 0$, while the spacing between E_k is of order g. Instead, phonons provide a thermal bath for electrons inducing transitions via thermal noise. Since $T_c \approx 0.18g$, at temperatures well below T_c the thermal energy T is much smaller than the typical spacing between the levels.

Consider several examples of scattering processes. A quasiparticle on level E_1 can interact with and break a Cooper pair resulting in three E_1 quasiparticles, $E_1 \to 3E_1$ and $2E_1/\Omega$ phonons. It can also absorb $N_{\rm ph} = (E_2 - E_1)/\Omega$ phonons and make a transition to level E_2, i.e., $E_1 \to E_2$. An E_2 particle can emit phonons and turn into an E_1 quasiparticle ($E_2 \to E_1$) or it can break a Cooper pair along the way resulting in three E_1 quasiparticles ($E_2 \to 3E_1$). Since the electron-phonon interaction [see, e.g., Eqs. (6) and (7)] can change the phonon number only by one at a time, all these processes have to go through multiple virtual states, e.g., $|E_2\rangle \to |E_1, 1\rangle \to |E_2, 2\rangle \to \ldots |E_1, N_{\rm ph}\rangle$, where we indicated the number of phonons at the second position in the ket vector. Intermediate states here are virtual and there are transitions with energy barriers of order g in any such process. Then, according to Kramer's rate theory [40–42] the quasiparticle decay (tunneling) rate for $T \ll g$ is

$$\Gamma_{\rm sc} = c_1 g e^{-c_2 g/T}, \tag{84}$$

where c_1 and c_2 are numerical coefficients of order one.

Now let λ be large but finite. We saw above that for such λ the energy level E_k broadens into a band of width Ω. It is natural to interpret this bandwidth as the uncertainty in the quasiparticle energy. Its inverse is then the quasiparticle lifetime and therefore the quasiparticle decay rate at low energies is

$$\Gamma_{\rm sc}^{\rm in} = \Omega = g\lambda^{-1/2}. \tag{85}$$

Equation (84) gives the rate of thermally activated transitions between different energy bands and Eq. (85)—the rate of transitions within a band. The total decay rate is the sum of the two:

$$\Gamma_{\rm sc}^{\rm tot} = c_1 g e^{-c_2 g/T} + g\lambda^{-1/2}. \tag{86}$$

Since $g/T_c \approx 5.5$, the second term dominates for all but extremely large λ. In any case, quasiparticle lifetime is very large at low energies. This again shows that there is a certain robustness, rigidity to the superconducting state. This state is not as manifestly unstable as the normal state.

V. QUALITATIVE PICTURE OF THE BREAKDOWN

Let us develop a more intuitive understanding of the breakdown of the Migdal-Eliashberg theory. We seek to explain vanishing quasiparticle lifetime and negative specific heat in the normal state at strong coupling and why the superconducting state is free of such pathologies. Of these two negative specific heat is especially important as it defines a value $\lambda_* \approx 3.69$ of the electron-phonon coupling above which the theory becomes invalid. We will see that the diverging quasiparticle decay rate is due to scattering of electrons from thermal fluctuations of static displacements of the ions (classical phonons), which have a natural interpretation as a disorder potential. The superconducting state is not affected by static disorder by Anderson's theorem.

The mechanics behind negative quasiparticle heat capacity is more sophisticated. We will see that this thermodynamic instability is driven by electrons near the Fermi surface interacting via quantum phonons (quantum fluctuations of the lattice). At $\lambda = \lambda_c$ the quasiparticle band structure changes abruptly and these electrons and quantum phonons lower their energy by forming new bound states. The Migdal-Eliashberg treatment does not capture the emergence of these new fermionic quasiparticles, but signals it via negative specific heat.

A. Quasiparticle decay rate

We found above that the quasiparticle decay rate in the normal state at strong electron-phonon coupling λ is

$$\Gamma_{\rm n} = \lambda\pi T. \tag{87}$$

There are two ways to interpret this result. First, it is important to realize that it is entirely due to electrons scattering from static displacements of the ions, which act as nonmagnetic impurities.

Consider the electron-phonon interaction term in the Holstein Hamiltonian (6),

$$H_{\text{el-ph}} = \sum_i (\alpha x_i) n_i. \tag{88}$$

At strong coupling, any finite temperature T is much larger than the frequency $\Omega \to 0$ of lattice oscillators. The oscillators are highly excited and therefore essentially classical. Their momenta p_i decouple and integrate out in the partition function. We are left with their coordinates x_i which are classical variables independent of the imaginary time τ—*classical phonons*. Therefore $\alpha x_i \equiv V_i$ in Eq. (88) is equivalent to a single-particle potential for the electrons. The problem is that of electrons moving in a random (due to thermal fluctuations of x_i) potential V_i. The potential comes at an elastic energy cost $\sum_i K x_i^2/2$, where K is the renormalized spring constant of the oscillators. The classical variable x_i coincides with its zeroth Matsubara component $x_i(0)$, i.e., with the imaginary time average $\bar{x}_i$,

$$x_i = \bar{x}_i \equiv x_i(0) = \frac{1}{\beta}\int_0^\beta d\tau\, x_i(\tau), \quad \beta = \frac{1}{T}, \tag{89}$$

since $x_i(\tau) = x_i$ is τ-independent. For this reason, we also refer to classical x_i as static displacements or classical phonons and use the notation $\bar{x}_i$ for them instead of x_i from now on to avoid confusion with the general quantum case. Note also that nonzero Matsubara components account for quantum fluctuations of ionic positions.

Quasiparticle decay rate due to nonmagnetic impurities is [16,43]

$$\Gamma_{\text{imp}} = \pi \nu_0 V^2. \tag{90}$$

The quantity V is the average strength of the disorder potential defined through

$$\sum_i \langle V_i(j) V_i(j')\rangle = V^2 \delta_{jj'}, \tag{91}$$

where $V_i(j)$ is the potential at site j produced by the impurity at i. In our case, $V_i(j) = \alpha \bar{x}_i \delta_{ij}$ and the average in Eq. (91) is the thermal average. We obtain

$$\Gamma_{\text{imp}} = \pi \nu_0 \alpha^2 \langle \bar{x}_i^2 \rangle_T. \tag{92}$$

By equipartition theorem for a classical harmonic oscillator, $K\langle \bar{x}_i^2\rangle_T = T$. Using this and the definition of λ in Eq. (11), $\lambda = \nu_0 \alpha^2/K$, we find that $\Gamma_{\text{imp}} = \lambda \pi T = \Gamma_{\text{n}}$. Therefore, to the leading order in the electron-phonon coupling λ, the quasiparticle decay rate in the normal state is due to electrons scattering from static displacements of the ions, or, in other words, from classical, zero Matsubara frequency phonons. Recall also that we previously obtained $\Gamma_{\text{n}} = \lambda \pi T$ from the $n = m$ term in Eq. (69), i.e., from the zero phonon frequency part of the self-energy.

Within this framework it is also easy to explain why the quasiparticle decay rate in the superconducting state remains negligible when at the same time it diverges in the normal state as $\lambda \to \infty$. The answer is that, as we know from Anderson's theorem [44], nonmagnetic disorder does not affect superconducting properties in conventional superconductors. This also explains the reason behind the cancellation of zero Matsubara frequency phonon ($\omega_n - \omega_m = 0$ term) from the Eliashberg gap equation (57a) and the free energy (25). Note that it is important here that the thermal averages $\langle x_i\rangle = 0$. The case of a regular pattern of nonzero $\langle x_i\rangle$ is not covered by Anderson's theorem.

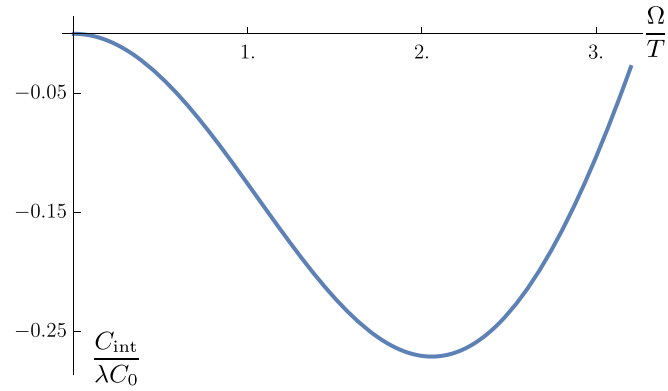

FIG. 4. Interaction contribution to the quasiparticle specific heat, C_{int} predicted by the Migdal-Eliashberg theory in units of λC_0, where C_0 is the specific heat of free fermions, λ is the electron-phonon coupling, and Ω is the natural frequency of the Einstein phonons. Note that $C_{\text{int}} < 0$ at any λ for all temperatures $T > \Omega/3$.

Another interpretation of Eq. (87) is as a rate of phonon emission and absorption in the limit of zero phonon frequency Ω. By Fermi's golden rule this rate is

$$\Gamma_{\text{ph}} = 2\pi \tilde{g}^2 \{n_B(\Omega)[1 - n_F(\Omega)] + [n_B(\Omega) + 1][1 - n_F(-\Omega)]\}\nu_0. \tag{93}$$

Here n_B and n_F are Bose and Fermi distributions and $\tilde{g} = \alpha/\sqrt{2M\Omega}$ is the electron-phonon interaction strength, which we obtain from Eq. (7) by setting $\alpha_{\boldsymbol{q}} = \alpha$ and $\omega_0(\boldsymbol{q}) = \Omega$. The first term in Eq. (93) corresponds to a fermion at the Fermi level $\varepsilon_F = 0$ absorbing a phonon of energy Ω and making a transition to the level Ω as long as that level is empty. The second term describes spontaneous plus simulated emission of a phonon by an electron at the Fermi level. Using $1 - n_F(-\Omega) = n_F(\Omega)$ and the definitions of g^2 and λ in Eqs. (9) and (11), we obtain the standard expression for inverse electron lifetime specialized to the case of Einstein phonons [38],

$$\Gamma_{\text{ph}} = \pi \lambda \Omega \{n_B(\Omega) + n_F(\Omega)\}. \tag{94}$$

When $\Omega/T \to 0$, the distributions $n_B(\Omega) \to T/\Omega$ and $n_F(\Omega) \to 1/2$. Therefore, in this limit, $\Gamma_{\text{ph}} = \lambda \pi T = \Gamma_{\text{n}}$ as claimed.

B. Negative specific heat

We derived the normal state specific heat C_n within the Migdal-Eliashberg theory in Sec. IV A, see Eq. (37). The contribution of the electron-electron interaction is

$$\frac{C_{\text{int}}}{C_0} = \lambda h\left(\frac{\Omega}{2\pi T}\right), \tag{95}$$

where $C_0 = \gamma_0 T$ is the noninteracting part and the total specific heat is $C_{\text{n}} = C_0 + C_{\text{int}}$. A plot of Eq. (95) is shown in Fig. 4. We see that C_{int} is negative as long as $T > \Omega/3$. It

is also proportional to λ, because the electron-electron interaction carries an overall factor of $g^2 \propto \lambda$, which corresponds to two electron-phonon vertices. Therefore $|C_{\rm int}|$ exceeds C_0 at any $T > \Omega/3$ for large enough λ, at which point the total specific heat becomes negative.

This instability is driven by *quantum* phonons, i.e., by quantum fluctuations of the ion displacements x_i. Phonons that determine the quasiparticle heat capacity are virtual and purely quantum because, as mentioned above, classical phonons sit at zero Matsubara frequency and their contribution—the $n = m$ term in Eq. (29)—cancels from the free energy. For this reason, this effect is more subtle than the divergence of the quasiparticle decay rate $\Gamma_{\rm n}$, which is entirely due to classical phonons. Note also that unlike negative specific heat, the linear growth of $\Gamma_{\rm n}$ does not provide a sharply defined value of λ above which the Migdal-Eliashberg theory loses validity.

Consider $\lambda = \infty$ for simplicity. In the spin language, negative quasiparticle heat capacity comes from the hard jump of the z component of spin (Fig. 2) combined with $\Omega = g\lambda^{-1/2} = 0$. It is these two factors that produce the divergent summation in Eq. (44) and the problematic $\ln T$ term in the normal state free energy. This term comes from interactions between antiparallel spins at $\omega_n > 0$ and $\omega_m < 0$ at distances $\omega_l = |\omega_n - \omega_m|$ of order $2\pi T$ from each other, since this contribution determines the lower limit of integration in Eq. (44). Therefore virtual phonons with frequencies of the order of $2\pi T$ and electrons with energies of the same order are responsible for the instability. In other words, the instability is due to interactions between electrons in a window of order $2\pi T \ll \varepsilon_F$ around the Fermi level mediated by quantum phonons.

Recall that S_n^z is proportional to an integral of the normal thermal Green's function (66) over $\xi_{\boldsymbol{p}}$. Since the Fermi energy is by far the largest energy scale, we integrate over $\xi_{\boldsymbol{p}}$ from $-\infty$ to $+\infty$ with a constant density of states. In the normal state, $\Phi_n = 0$ and the integration gives $S_n^z = \mathrm{sgn}(\omega_n + \Sigma_n) = \mathrm{sgn}(\omega_n)$. In the superconducting state, the same integration obtains

$$S_n^z = \frac{\omega_n + \Sigma_n}{\sqrt{(\omega_n + \Sigma_n)^2 + |\Phi_n|^2}} = \frac{\omega_n}{\sqrt{\omega_n^2 + \Delta_n^2}}, \tag{96a}$$

$$S_n^x = \frac{\Delta_n}{\sqrt{\omega_n^2 + \Delta_n^2}}. \tag{96b}$$

Below T_c, spins acquire x components softening the jump in S_n^z. This deviation of spins from the z axis increases their ferromagnetic interaction energy resulting in a discontinuity in the specific heat, such that it becomes positive in the superconducting state as we found in Sec. IV B. In this way, opening of the superconducting gap removes the instability.

We saw in the previous section that classical ion displacements $\bar{x}_i$ provide a fluctuating single-particle potential $V_i = \alpha\bar{x}_i$ for the electrons. Nonzero thermal averages of $\bar{x}_i$ mean a nonzero average potential V_i, which modifies the electronic band structure. In particular, as we discuss in more detail in Sec. IX, it can open a gap Δ_P at the Fermi level via the Peierls mechanism. This metal-insulator transition stabilizes the system like the opening of the superconducting gap. Indeed, suppose $\xi_{\boldsymbol{p}}^2 = \eta_{\boldsymbol{p}}^2 + \Delta_{\boldsymbol{p}}^2$. Now the integration of Eq. (66) over $\eta_{\boldsymbol{p}}$ from $-\infty$ to $+\infty$ in the normal state ($\Phi_n = 0$) gives

$$S_n^z = \frac{\omega_n + \Sigma_n}{\sqrt{(\omega_n + \Sigma_n)^2 + \Delta_P^2}}. \tag{97}$$

We see that the band gap Δ_P plays a role similar to the anomalous average $|\Phi_n|$. Following the same steps as before [14] but for a gapped single-particle spectrum, we derived the spin chain representation for the free energy for this case. The part involving S_n^z is the same as in Eq. (29) but with S_n^z from Eq. (97). In addition, there is an infinite range ferromagnetic $S_n^x S_m^x$ interaction. Stronger ferromagnetism suggests that spectral gap opening precedes the superconducting transition in agreement with our finding that the specific heat becomes negative above the superconducting T_c.

It is possible that a soft gap or a pseudogap may stabilize the electron-phonon system as well. However, we show in Sec. IX that at least for certain system parameters a hard gap Δ_P (metal-insulator transition) is preferred. In any case, a substantial depression of the density of states near the Fermi energy at $\lambda > \lambda_c$ is necessary to remove the negative specific heat pathology. Other changes of the band structure, such as band narrowing etc., are insignificant near λ_c given that the Fermi energy is still much larger than all other energies. Even though we discussed classical phonons separately for the sake of the argument, the effect of quantum phonons on the quasiparticle spectrum is equally important and inseparable from that of classical phonons.

Now we are in a position to explain the breakdown of the Migdal-Eliashberg theory signaled by the negative specific heat. At λ_c the nature of fermionic quasiparticles changes abruptly. Electrons near the Fermi surface and quantum phonons lower their energy by forming new bound states—new quasiparticles with gapped spectrum. This transition involves both quantum and classical phonons. Quantum phonons dress the electrons and classical phonons facilitate the gap opening. Suppose we prepare the system in the Migdal-Eliashberg normal state at $\lambda > \lambda_c$ and "temperature" T. Here T is a parameter rather than the true temperature as this state is not the true thermal equilibrium. Next, we bring the system into contact with a thermal bath at temperature $T + \delta T > T$ and allow it to equilibrate. Since there are new quasiparticle states with lower energies available, some of the Migdal-Eliashberg quasiparticles transition into these new states. The total energy decreases as the system equilibrates, i.e., the heat capacity is negative.

VI. NEW PHASE TRANSITION

We showed that the specific heat of the Migdal-Eliashberg normal state is negative in a range of temperatures, $T_c < T < T_+$, at strong electron-phonon coupling, $\lambda > \lambda_* \approx 3.7$. Therefore this state is no longer the global minimum of the free energy. New order must emerge above certain λ_c, such that $3.0 \leqslant \lambda_c \leqslant 3.7$, see Eq. (48). Considerations of the preceding section suggest that ion displacements acquire site-dependent averages $\langle x_i \rangle$ breaking lattice translational invariance in the emergent phase. We also saw that $V_i = \alpha x_i$ plays the role of a disorder potential. As λ increases, the strength of the disorder $\alpha \propto \sqrt{\lambda}$ increases with it. This again suggests a

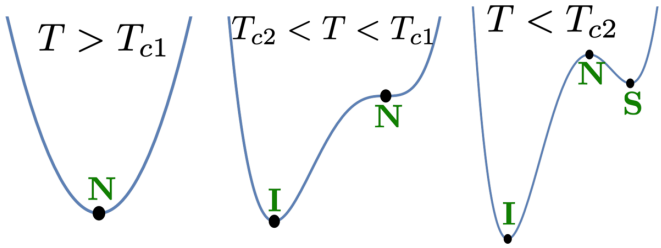

FIG. 5. Schematic plot of the free energy of the electron-phonon system illustrating the emergence of a new global minimum at strong coupling, $\lambda > \lambda_c$. This minimum is either an insulator or a Fermi liquid with broken translational invariance; we take it to be an insulator for definiteness. At $T > T_{c1}$, the system is in the normal (N) state. At T_{c1}, insulating (I) order develops. As we decrease the temperature further, the superconducting (S) stationary point emerges at $T = T_{c2}$ as a local minimum or a saddle point. At temperatures just below T_{c2}, this stationary point must be higher in energy than the insulator.

metal-insulator transition. Indeed, we find in Sec. IX that in the adiabatic limit at half filling the system is an insulator for $\lambda > \lambda_c$. By continuity we expect this to persist at least to some extent into the nonadiabatic regime, see also Ref. [10]. Another candidate for the new order is a Fermi liquid with broken lattice translational invariance. Whether the new global minimum is an insulator or such a Fermi liquid depends on factors unimportant in standard Migdal-Eliashberg treatment, such as the filling fraction and lattice symmetry. We assume it is an insulator in this section for definiteness.

When $\lambda < \lambda_c$, the system undergoes a metal-superconductor transition at $T_c \equiv T_{c2}$ described by the Migdal-Eliashberg theory. At fixed $\lambda > \lambda_c$, the new phase transition occurs at a certain critical temperature $T_{c1} > T_+ > T_{c2}$. At very high temperatures, the system is in the normal state (a classical gas of fermions and phonons). The superconducting stationary point develops below T_{c2} as a local minimum or a saddle point, since the Eliashberg gap equation has a nontrivial solution below T_{c2} for all λ. The superconducting state cannot be the global minimum just below T_{c2}, because it is close in energy to the normal state, while the insulating state is already far, see Fig. 5. Nevertheless, as we continue to lower the temperature, the superconductor can still prevail over the insulator via a first-order phase transition.

One more consequence of the emergence of the new global minimum is that there must be a first-order phase transition as a function of λ for certain temperatures below T_{c2}. We saw that there must be a range of temperatures below T_{c2} where the system is an insulator for $\lambda > \lambda_c$. As we decrease λ below λ_c, the electron-phonon system switches from a well-formed insulating global minimum to a well-formed superconducting minimum. This is only possible through a first-order phase transition.

VII. COMPARISON TO OTHER STUDIES

There are numerous publications discussing the breakdown of the Migdal-Eliashberg theory at strong coupling, see, e.g., Refs. [5–11]. However, none of them demonstrate a true breakdown, i.e., show that the theory loses validity when the coupling λ exceeds a certain finite value. Rather than testing the validity of the Migdal-Eliashberg theory within its domain of applicability, most studies rediscover the lattice instability pointed out by Migdal and Eliashberg [1,2] or explore the post-instability physics to which the theory no longer applies, see also the discussion in Introduction.

In conventional electron-phonon models, such as the Frölich and Holstein Hamiltonians, electron-phonon interactions renormalize the phonon frequencies approximately as [1,2,17]

$$\omega_q \approx \omega_0(q)\sqrt{1-2\lambda_0}, \tag{98}$$

where λ_0 is the *bare* electron-phonon coupling constant defined by the same Eq. (11) as λ, but with $\Omega \to \Omega_0$ and $\omega_q \to \omega_0(q)$. It follows from Eq. (11) that the *renormalized* dimensionless electron-phonon coupling is

$$\lambda = \frac{\lambda_0}{1-2\lambda_0}. \tag{99}$$

Equations (98) and (99) are one-loop renormalization equations. They hold for both Holstein (6) and the more general Hamiltonian (7) in 2D and 3D [16,45]. In infinite dimensional space [46], $1-2\lambda_0$ is replaced with $1-\frac{8}{3}\lambda_0$ in Eqs. (98) and (99).

More accurate renormalization equations are available, but they do not change the fact that the lattice loses stability at a certain $\lambda_0 = \lambda_{\mathrm{LI}}$ and that the renormalized coupling λ grows monotonously with λ_0 and diverges at $\lambda_0 = \lambda_{\mathrm{LI}}$. Our analysis does not depend on the value of λ_{LI} and for concreteness we take $\lambda_{\mathrm{LI}} = 0.5$. As mentioned in Introduction, this lattice instability is merely an artifact of the conventional models. It is nevertheless very real in studies of such models that do not take precautions to factor it out as we did in this paper.

Main assumptions of the Migdal-Eliashberg theory are that the electron-phonon system is metallic and translationally invariant. None of these are guaranteed past the lattice instability, which changes lattice symmetry and may, for example, open a gap at the Fermi surface through the Peierls mechanism, which we discuss in Sec. IX. It is for this reason that Migdal and Eliashberg restricted [1,2,17] their theory to $\lambda_0 \leqslant 0.5$. Note also that an early textbook account of this theory [16], which closely follows the original work, makes it clear on p. 182 that η (our λ_0) should not be "too close to 1/2."

Equation (99) shows that the *entire domain* of the theory, $0 \leqslant \lambda \leqslant \infty$, maps to the interval $0 \leqslant \lambda_0 \leqslant 0.5$. Asserting its breakdown past the lattice instability is tautological as such values of λ_0 are already outside of its domain of applicability. A meaningful statement would be that it breaks down at a finite λ, which then maps to a certain $\lambda_0 < 0.5$, see also Ref. [47]. Prior work mixes up the true breakdown of the Migdal-Eliashberg theory with the lattice instability. As a result, it does not eliminate the possibility that the theory remains valid for all λ, including $\lambda = \infty$. This, for example, leaves the door open to the hypothesis [19] that the strong coupling, $\lambda \to \infty$, limit of the Migdal-Eliashberg theory is realized in the Holstein model when $\lambda_0 \to 0.5$ underscoring the luck of conclusiveness of the prior work. In contrast, our study eliminates this hypothesis.

The confusion stems in part from misunderstanding of Migdal's theorem. This theorem is often interpreted as follows: the Migdal-Eliashberg theory is valid provided the parameter $\lambda_0\Omega_0/\varepsilon_F$ is small (for dispersing phonons, we replace Ω_0 with the maximum phonon frequency). This statement is incorrect. This form of the Migdal parameter assumes $T = 0$ and λ_0 not too close to 0.5 (no substantial renormalization, i.e., $\lambda \sim \lambda_0$). The proper zero temperature Migdal parameter, suitable for all λ, uses renormalized coupling and phonon frequency,

$$x_M = \frac{\lambda\Omega}{\varepsilon_F}. \tag{100}$$

Most importantly, Migdal's theorem is a *local* statement about the Eliashberg stationary point [18]. It says that *quadratic* fluctuations of the Eliashberg fields Σ_σ and Φ around this point are small. This makes the stationary phase approximation—the Migdal-Eliashberg theory—accurate *when* it is the global minimum of the free energy. But it is meaningless to apply Migdal's theorem as well as the Migdal-Eliashberg theory when the global minimum is something else, e.g., an insulator, see Fig. 5.

Moreover, it is not even clear how to evaluate x_M at the "wrong" minimum and what is its significance there. For example, what are the renormalized coupling and phonon frequencies past the lattice instability? The Fermi energy ε_F plays a different role in an insulator compared to a metal. At the same time, Migdal's theorem as formulated above *remains valid* when applied at the Eliashberg stationary point even when this point is no longer the global minimum. However, we have to keep in mind that now this stationary point is not relevant to the equilibrium physics.

Consider, for instance, an impressive Monte Carlo study of the square-lattice Holstein model [10]. This study reports that the deviation of the s-wave pair susceptibility from its Eliashberg value grows from roughly 1% to 25% as λ_0 increases from 0.4 to 0.5. A part of this deviation must be due to the Migdal parameter (100) being finite. Not only is x_M nonzero, but it also diverges as $(1 - 2\lambda_0)^{-1/2}$ as we approach $\lambda_0 = 0.5$, though finite T cuts off this divergence [18]. Another contribution is the finite size effect, which turns the sharp transition at $\lambda_0 = 0.5$ present in the Holstein model into a crossover over a certain interval of λ_0 around 0.5. Without knowing the magnitude of these contributions to the deviation, it is impossible to tell whether or not it indicates true breakdown of the theory.

Our analysis is very different from previous work. We showed that the Migdal-Eliashberg theory breaks down at a finite value of the electron-phonon coupling λ independently of the underlying microscopic electron-phonon model. We based this conclusion on an unambiguous marker of the breakdown—negative specific heat. Our value $\lambda_* \approx 3.69$ where the specific heat becomes negative translates into $\lambda_0 \approx 0.44$ according to Eq. (99). This appears close to $\lambda_0 \approx 0.4$ reported in Ref. [10] as the point where the determinant Monte Carlo computation starts to deviate from the Migdal-Eliashberg prediction. However, it is important to keep in mind that the entire strong coupling regime of the Eliashberg theory maps to the left vicinity of $\lambda_0 = 0.5$. Because of this and without knowing the systematic error on the number 0.4 it is difficult to draw any conclusion from its proximity to our result.

VIII. CLASSICAL PHONONS

We saw that static deformations $\bar{x}_i$ of the lattice (zero Matsubara frequency phonons) facilitate the breakdown of the Migdal-Eliashberg theory. They provide a statistically distributed single-particle potential $V_i = \alpha\bar{x}_i$ for the electrons, where $\alpha \propto \sqrt{\lambda}$. To understand this better, consider the strong coupling limit, $\lambda \to \infty$, of this theory. Recall the definition of the electron-phonon coupling λ for the Holstein model,

$$\lambda = \frac{g^2}{\Omega^2} = \frac{\nu_0\alpha^2}{K}. \tag{101}$$

We see that the strong coupling limit is the *free ion limit*—the limit where the spring constant K of lattice oscillators vanishes. As K decreases, nonuniform thermal averages of $\bar{x}_i$ come at lower and lower elastic energy cost, while the strength of the potential V_i keeps increasing. Inevitably, at a certain point it becomes energetically favorable to generate a nonuniform average potential V_i for the electrons.

Euclidian Lagrangian corresponding to the Holstein Hamiltonian (6) is

$$L = \sum_{ij,\sigma} c^*_{i\sigma} G^{-1}_{0ij} c_{j\sigma} + \sum_i \left[\frac{K x_i^2}{2} + \frac{M(\partial_\tau x_i)^2}{2}\right] + \alpha \sum_{i\sigma} c^*_{i\sigma} c_{i\sigma} x_i. \tag{102}$$

The fields $c^*_{i\sigma}$, $c_{i\sigma}$, and x_i depend on the imaginary time τ, $G^{-1}_{0ij} = \partial_\tau\delta_{ij} + t_{ij} - \mu\delta_{ij}$, and we replaced the arbitrary single-particle Hamiltonian h_{ij} with a translationally invariant hopping matrix t_{ij} and the bare spring constant K_0 with the renormalized constant K. The action in the Matsubara frequency representation reads

$$S = \sum_{ij,n\sigma} c^*_{i\sigma}(n) G^{-1}_{0ij} c_{j\sigma}(n) + \frac{M}{2}\sum_i \left[\Omega^2 + \omega_l^2\right] x_i^2(l) + \alpha \sum_{i\sigma} c^*_{i\sigma}(n+l) c_{i\sigma}(n) x_i(l), \tag{103}$$

where now

$$G^{-1}_{0ij} = -i\omega_n\delta_{ij} + t_{ij} - \mu\delta_{ij}, \tag{104}$$

and n and l stand for fermionic and bosonic Matsubara frequencies ω_n and ω_l, respectively.

Integrating out the phonon field $x_i(l)$, we obtain the effective electron-electron interaction (9) for the Holstein model, namely,

$$\lambda(\omega_l) = \frac{g^2}{\omega_l^2 + \Omega^2}. \tag{105}$$

In the strong coupling limit, $\Omega = 0$ and the interaction blows up at $\omega_l = 0$, $\lambda(\omega_l = 0) = \lambda \to \infty$. This divergence propagates into the normal self-energy Σ_n and gives rise to the divergent imaginary part of the pole of the retarded Green's function (71). This $\omega_l = 0$ part (zero Matsubara frequency phonons) of the interaction is responsible for the divergence of the quasiparticle decay rate, as we already saw above.

This divergence arises from integrating out $\omega_l = 0$ phonons, because this is illegal in the strong coupling limit. In this limit, $\Omega = 0$ and $x_i^2(0)$ term is absent from the action (103). The integral over $x_i(0)$ is no longer Gaussian and this field therefore cannot be integrated out. Instead, we incorporate the $\alpha \sum_{i\sigma} c^*_{i\sigma}(n)c_{i\sigma}(n)x_i(0)$ term in Eq. (103) into the single-fermion part by replacing the hopping t_{ij} in Eq. (104) with

$$h_{ij} = t_{ij} + \alpha \bar{x}_i, \tag{106}$$

where

$$\bar{x}_i \equiv x_i(0) = \frac{1}{\beta}\int_0^\beta d\tau\, x_i(\tau), \quad \beta = \frac{1}{T}. \tag{107}$$

We see again that static displacements of the ions provide an on-site potential for the electrons. We also discussed in Sec. V A that variables $\bar{x}_i$ are classical displacement fields (classical phonons).

IX. ADIABATIC LIMIT

To gain further insight into post-Migdal-Eliashberg physics, consider the adiabatic limit where the ion mass $M \to \infty$. This limit is complimentary to the strong coupling limit $K \to 0$. All phonons are classical in the adiabatic limit and their role becomes especially transparent. Studies of polarons, bipolarons etc. frequently employ this limit as it is much simpler than dealing with quantum phonons [5,7,10,15]. In this limit, $g = 0$ and the electron-electron interaction (9) vanishes for all $\omega_l \neq 0$.

The Holstein Hamiltonian (6) becomes at $M = \infty$,

$$H = \sum_{ij\sigma} t_{ij} c^\dagger_{i\sigma} c_{j\sigma} + \sum_i \frac{K_0 x_i^2}{2} + \alpha \sum_i n_i x_i, \tag{108}$$

where we replaced the arbitrary h_{ij} with a translationally invariant hopping matrix t_{ij}. Note that the dimensionless electron-phonon coupling (11),

$$\lambda_0 = \frac{\nu_0 \alpha^2}{K_0}, \tag{109}$$

remains finite in this limit [48]. We use unrenormalized version of Eq. (11), because there is no renormalization in the usual sense in the adiabatic limit (see below). Ion displacements x_i now commute with the Hamiltonian, which allows us to treat them as classical variables. However, they do not commute with the total momentum operator $\boldsymbol{P}$ and the commutation relations,

$$[x_i, H] = [\boldsymbol{P}, H] = 0, \quad [x_i, \boldsymbol{P}] \neq 0, \tag{110}$$

imply that the eigenstates of the Hamiltonian are degenerate [49].

Consider the Holstein Hamiltonian (108). We are to find a lattice distortion x_i that minimizes the energy. Suppose we observe that initially uniform x_i (independent of i) become nonuniform as we increase α. This is known as Peierls or, more generally, charge density wave (CDW) instability [12,13]. Peierls distortion lowers the energy by opening a gap at the Fermi surface resulting in a metal-insulator transition. In 1D the CDW wave vector is $2p_F$—twice the Fermi momentum. In 2D, we expect the CDW wave vectors to depend on the geometry of the Fermi surface as well. The Fourier transform of x_i can now contain more than one Fourier mode unlike in 1D.

CDW instability in dimensions higher than one is a more complicated matter. 1D Fermi surface is perfectly nested at $2p_F$. The closest 2D analog in the Holstein model (108) is a square lattice at half filling with nearest neighbor hopping. Then, the Fermi surface is a square nested at $\boldsymbol{Q} = (\pi, \pi)$ and we expect this to be the dominant CDW wave vector. Commensurate (π, π) CDW has been found in a very similar model at 0.4 filling [10], but it could be difficult to differentiate numerically between (π, π) and nearby wave vectors on a small lattice. And in any case there is no reason to expect pure commensurate (π, π) CDW away from half filling. Even at half filling, there is an admixture of other wave vectors in the CDW [50].

Nevertheless, let us take the (π, π) lattice distortion pattern

$$x_i = X_{\text{c.m.}} + (-1)^{i_x + i_y}\delta x. \tag{111}$$

as our variational wave function. The center of mass displacement $X_{\text{c.m.}}$ couples only to the total fermion number. At the minimum, $X_{\text{c.m.}} = -\alpha/K_0$. The Hamiltonian for the remaining degrees of freedom in the momentum representation is

$$\begin{aligned} H =& \frac{1}{2}\sum_{\boldsymbol{k}\sigma}[\varepsilon_{\boldsymbol{k}} c^\dagger_{\boldsymbol{k}\sigma} c_{\boldsymbol{k}\sigma} + \varepsilon_{\boldsymbol{k}+\boldsymbol{Q}} c^\dagger_{\boldsymbol{k}+\boldsymbol{Q},\sigma} c_{\boldsymbol{k}+\boldsymbol{Q},\sigma} \\ &+ \Delta_P c^\dagger_{\boldsymbol{k}\sigma} c_{\boldsymbol{k}+\boldsymbol{Q},\sigma} + \Delta_P c^\dagger_{\boldsymbol{k}+\boldsymbol{Q},\sigma} c_{\boldsymbol{k}\sigma}] + \frac{\nu_0 N \Delta_P^2}{2\lambda_0}, \end{aligned} \tag{112}$$

where $\Delta_P = \alpha\delta x$ is the Peierls gap.

It is straightforward to diagonalize this Hamiltonian by a Bogoliubov transformation:

$$H = \frac{1}{2}\sum_{\boldsymbol{k}\sigma} E_{\boldsymbol{k}}(a^\dagger_{\boldsymbol{k}\sigma+} a_{\boldsymbol{k}\sigma+} - a^\dagger_{\boldsymbol{k}\sigma-} a_{\boldsymbol{k}\sigma-}) + \frac{\nu_0 N \Delta_P^2}{2\lambda_0}, \tag{113}$$

where $(a^\dagger_{\boldsymbol{k}\sigma\pm}, a_{\boldsymbol{k}\sigma\pm})$ are the new quasiparticles and $E_{\boldsymbol{k}} = \sqrt{\varepsilon_{\boldsymbol{k}}^2 + \Delta_P^2}$. The Hamiltonian (113) is nearly identical to the mean-field BCS Hamiltonian. Minimizing the total energy with respect to Δ_P, we obtain a version of the BCS gap equation

$$\int_{\varepsilon_<}^{\varepsilon_F} \frac{\Delta_P d\varepsilon}{\sqrt{\varepsilon^2 + \Delta_P^2}} = \frac{\Delta_P}{\lambda_0}, \quad \varepsilon_< = \varepsilon_F|1 - 2\mathsf{f}|, \tag{114}$$

where f is the filling fraction. For simplicity, we took the density of states to be constant as its energy dependence is unimportant for our discussion.

As usual, $\Delta_P = 0$ is always a solution of the gap equation. A nonzero solution, when it exists, is always the minimum of the energy. At half filling, $\varepsilon_< = 0$ and the Peierls gap $\Delta_P = \varepsilon_F e^{-1/\lambda_0}$ opens already at $\lambda_0 = 0^+$. Away from the half filling, the gap opens at $\lambda_0^c = -(\ln|1 - 2\mathsf{f}|)^{-1}$ for this lattice distortion pattern [51]. The transition is always second order, even though numerically it is easy to mistake it for the first-order transition [10] due to a rapid rise of Δ_P past λ_0^c for certain choices of parameters.

In this example, the metal-insulator transition occurs at $\lambda_0^c = 0^+$, because the conditions for it are ideal: frozen lattice vibrations and nested Fermi surface. The Migdal-Eliashberg theory applies only at $\lambda_0 = 0$ in this setup. In other circumstances, the transition shifts to nonzero λ_0. In the adiabatic limit, the phonon mediated electron-electron interaction is extremely retarded, $\lambda_{\rm nm} = \lambda\delta_{nm}$. Eq. (57a) then implies that the gap function vanishes. The electron Green's function is given by Eq. (71) now for all T, because $T_c = 0$. Notice that it reproduces exact energy levels of the Hamiltonian (108) for $\lambda_0 < \lambda_0^c$ when $x_i = \text{const}$. Therefore the Migdal-Eliashberg theory is exact at $T = 0$ in the metallic phase, though this phase is confined to $\lambda_0 = 0$.

Renormalization equations discussed in Introduction do not work in the adiabatic limit, since $\Omega_0 = 0$ and the phonon propagator vanishes at all but zero frequency. Temperature-dependent renormalization of the spring constant K_0 and λ_0 with it can occur, but we do not investigate it here. Most importantly, this example confirms once more that the role of the classical phonons is to modify the single-fermion spectrum.

X. LATTICE-FERMIONIC SUPERFLUIDITY

We saw that classical (zero Matsubara frequency) phonon field $x_i(0)$ provides a statistically distributed potential $V_i = \alpha x_i(0)$ for the electrons. As α grows, $x_i(0)$ acquire nonzero thermal averages. The resulting single-particle potential V_i together with dressing of fermions by quantum phonons lead to abrupt changes in the fermion band structure. Examples include gap opening at the Fermi level resulting in a superconductor-insulator transition and polaronic Fermi liquid at low densities. At even stronger electron-phonon interaction, dramatic band narrowing and Bose-Einstein condensation of bipolorons [7] can occur.

In this section, we construct a theory which treats the classical phonons properly. At not too large electron-phonon coupling λ, it reduces to the Migdal-Eliashberg theory, and in the adiabatic limit it reduces to the polaron formation theory, which predicts electron localization in 2 and 3D for $\lambda_0 \gtrsim 1$ [15]. It also reproduces the results of the previous section for the half-filled Holstein model on square lattice in the adiabatic limit. It continues to work past λ_c where the Eliashberg theory breaks down and describes at least some of the new phases that emerge at $\lambda > \lambda_c$. We dub this theory lattice-fermionic superfluidity, because it potentially encompasses several superfluid phases and because the lattice (quantum and classical phonons) and the fermions are much closer intertwined in this theory than in the theory of conventional superconductivity. However, we stress that our theory is meant to describe non-superfluid phases, such as a metal or an insulator, as well.

Our starting point is the action (103) for the Holstein model, where t_{ij} has been replaced with h_{ij} given by Eq. (106). In the previous paper [14], we determined the effective action and a *spatially nonuniform* version of the Eliashberg stationary point for the Holstein model with an *arbitrary* single-electron Hamiltonian h_{ij} (see Appendix A 3 of Ref. [14]) and used it to map the free energy to a classical spin chain. The approach is similar to the one outlined in Sec. II B, except we now do not assume translational invariance and work in the eigenbasis of an arbitrary h_{ij}.

The derivation of the theory of lattice-fermionic superfluidity goes through the same steps except (a) the effective electron-electron interaction now excludes $\omega_l = 0$, because we do not integrate out $\bar{x}_i \equiv x_i(0)$, and (b) we need to minimize with respect to the new parameters $\bar{x}_i$. We obtain the following effective action [cf. Eq. (8)]:

$$\begin{aligned} S_{\rm eff} = T\nu_0 \sum_{nl\alpha} \big[&\big(\Phi^\alpha_{n+l}\big)^* \Lambda_l \Phi^\alpha_n + \Sigma^\alpha_{n+l}\Lambda_l\Sigma^\alpha_n \\ &- \chi^\alpha_{n+l}\Lambda_l\chi^\alpha_n\big] - \sum_{n\alpha} \ln\big[\big(\omega_n + \Sigma^\alpha_n\big)^2 + \big|\Phi^\alpha_n\big|^2 \\ &+ \big(\chi^\alpha_n + \xi_\alpha\big)^2\big] + \frac{K_0}{2T}\sum_i \bar{x}_i^2, \end{aligned} \tag{115}$$

Here Φ^α_n, Σ^α_n, and χ^α_n are the components of the three fields $\Phi_i(\tau', \tau)$, $\Sigma_{i\uparrow}(\tau', \tau)$, and $\Sigma_{i\downarrow}(\tau', \tau)$ with which we decoupled the four-fermion term after integrating out the phonons. On the stationary point, the fields depend only on the difference $\tau' - \tau$. Let $\Sigma_{in\uparrow}$ be the Fourier transform of $\Sigma_{i\uparrow}(\tau' - \tau)$ with respect to $\tau' - \tau$. We define $\Sigma^\alpha_{\uparrow n}$ as

$$\Sigma^\alpha_{\uparrow n} = \sum_i \pi^*_{i\alpha}\Sigma_{in\uparrow}\pi_{i\alpha}, \tag{116}$$

and similarly for the other fields. Here $\pi_{i\alpha}$ are the eigenstates of $h_{ij} = t_{ij} + \alpha\bar{x}_i\delta_{ij}$, i.e.,

$$\sum_j [t_{ij} + \alpha\bar{x}_i\delta_{ij}]\pi_{j\gamma} = \varepsilon_\gamma\pi_{i\gamma}, \tag{117}$$

and $\xi_\gamma = \varepsilon_\gamma - \mu$. The fields Σ^α_n and χ^α_n are defined through

$$\Sigma^\alpha_n = \frac{\Sigma^\alpha_{\uparrow n} - \Sigma^\alpha_{\downarrow,-n}}{2}, \quad i\chi^\alpha_n = \frac{\Sigma^\alpha_{\uparrow n} + \Sigma^\alpha_{\downarrow,-n}}{2}. \tag{118}$$

We retain unrenormalized spring constant K_0 for the classical phonons.

We need to minimize the effective action (115) with respect to the real fields $\bar{x}_i$, Σ_{in}, and χ_{in} and complex field Φ_{in}. Minimizing with respect to the latter three fields, we obtain three generalized Eliashberg equations [14]:

$$\begin{aligned} \sum_\gamma \Phi^\gamma_n|\pi_{i\gamma}|^2 &= T\sum_{m\neq n,\gamma}\frac{\lambda_{\rm nm}}{\nu_0}\frac{\Phi^\gamma_m|\pi_{i\gamma}|^2}{\Theta^\gamma_m}, \\ \sum_\gamma \Sigma^\gamma_n|\pi_{i\gamma}|^2 &= T\sum_{m\neq n,\gamma}\frac{\lambda_{\rm nm}}{\nu_0}\frac{\big(\omega_m + \Sigma^\gamma_m\big)|\pi_{i\gamma}|^2}{\Theta^\gamma_m}, \\ \sum_\gamma \chi^\gamma_n|\pi_{i\gamma}|^2 &= -T\sum_{m\neq n,\gamma}\frac{\lambda_{\rm nm}}{\nu_0}\frac{\big(\xi_\gamma + \chi^\gamma_m\big)|\pi_{i\gamma}|^2}{\Theta^\gamma_m}, \end{aligned} \tag{119}$$

where $\Theta^\gamma_m = (\omega_m + \Sigma^\gamma_m)^2 + |\Phi^\gamma_m|^2 + (\chi^\gamma_m + \xi_\gamma)^2$, $\lambda_{\rm nm} = \lambda(\omega_n - \omega_m)$ is given by Eq. (9) as before. The renormalized frequency Ω in Eq. (9) is an *independent parameter* not fixed by the theory.

To minimize Eq. (115) with respect to $\bar{x}_i$, we use

$$\frac{\partial\xi_\gamma}{\partial\bar{x}_i} = \frac{\partial\varepsilon_\gamma}{\partial\bar{x}_i} = \alpha|\pi_{i\gamma}|^2, \tag{120}$$

which follows from the first order of the perturbation theory in $\delta\bar{x}_i$. Note that the chemical potential μ in $\xi_\gamma = \varepsilon_\gamma - \mu$ is a Lagrange multiplier that does not depend on $\bar{x}_i$ until

later, when we fix the average electron number. Setting the derivative of the effective action with respect to $\bar{x}_i$ to zero, we find

$$K_0\bar{x}_i = -2\alpha\sum_\gamma n_\gamma|\pi_{i\gamma}|^2, \tag{121}$$

where n_γ are the occupation numbers,

$$n_\gamma = \frac{1}{2} - T\sum_m \frac{\xi_\gamma}{\left(\omega_m + \Sigma_m^\gamma\right)^2 + \left|\Phi_m^\gamma\right|^2 + \xi_\gamma^2}. \tag{122}$$

We derived this expression with the help of the normal Green's function (66) generalized to the case of nonuniform self-energies (replace $\boldsymbol{p}$ with γ and Σ_n and Φ_n with Σ_n^γ and Φ_n^γ). The average electron number $N_e = \sum_\gamma 2n_\gamma$ determines the chemical potential.

Substituting $\bar{x}_i$ from Eq. (121) back into Eq. (117), we arrive at a discrete nonlinear Schrödinger equation where the potential is a weighted sum of $|\pi_{i\gamma}|^2$ over all states:

$$\sum_j t_{ij}\pi_{j\gamma} - 4E_b\pi_{i\gamma}\sum_\delta n_\delta|\pi_{i\delta}|^2 = \varepsilon_\gamma\pi_{i\gamma}. \tag{123}$$

Here $E_b = \frac{\alpha^2}{2M\Omega_0^2} = \frac{\lambda_0}{2\nu_0}$ has the meaning of the polaron binding energy [52]. Together with Eqs. (119) we have four coupled equations for four unknowns: $\pi_{i\gamma}$, ε_γ, Φ_n^γ, Σ_n^γ, and χ_n^γ.

These equations have several kinds of solutions. First, there is always the solution where $\pi_{i\gamma}$ are plane waves. In this case, $\alpha x_i = \bar{\mu}$ is spatially uniform and reduces to a shift of the chemical potential, $\mu \to \mu - \bar{\mu}$ in Eqs. (119). And conversely, if $\bar{x}_i$ does not break the translational symmetry of the lattice, i.e., is i-independent, $\pi_{i\gamma}$ are plane waves. Then, the fields $\Phi_n^\gamma \equiv \Phi_n$, $\Sigma_n^\gamma \equiv \Sigma_n$, and $\chi_n^\gamma \equiv \chi_n$ are independent of the index γ and summing over it, we end up with the Eliashberg equations generalized to the non-particle-hole-symmetric case (Eq. (A.18) in Ref. [14]), except $m = n$ terms are absent from the summations. But as we mentioned above, this is an an alternative way to write the Eliashberg equations. Indeed, we showed in Ref. [14] that Eqs. (13) and Eqs. (18) are equivalent. The same applies to the more general Eliashberg equations for the fields Σ_n, Φ_n, and χ_n.

Now consider the adiabatic limit. In this limit, $\lambda_{\rm nm} = 0$ for $m \neq n$ and only the nonlinear Schrödinger equation (123) is left. This equation describes polarons in 1D, 2D, and 3D, see Ref. [15] and references therein. Setting additionally $T = 0$, we see that Eq. (123) is the exact minimization condition for the Holstein Hamiltonian (108) from which we deduced that the system becomes a CDW insulator for $\lambda_0 > \lambda_0^c$. Therefore the lattice-fermionic theory remains valid long after the Eliashberg theory breaks down and is exact in the adiabatic limit for any value of λ_0, at least at $T = 0$.

As the strength of the electron-phonon interaction α grows, the potential in Eq. (123) becomes stronger. The electron effective mass grows and the band narrows. The band narrowing is exponential in $-E_b/\Omega_0$ [53,54]. In the narrow band regime, Eq. (123) supports self-trapping of fermions (polarons). Indeed, consider the flat band limit for simplicity. Let $\pi_{i\gamma} = \delta_{i\boldsymbol{\gamma}}$ be a state where the fermion is at site $\boldsymbol{\gamma}$. We see that by occupying certain sites, the fermions make the potential (121) deeper at these sites thus lowering their energy. In this regime, solutions of Eqs. (123) and (119) are well outside of the Migdal-Eliashberg theory. The system of equations (123) and (119) is more complex than the Eliashberg gap equation (57a). Nevertheless, it is still solvable in a polynomial time as the number of equations and unknowns is polynomial in the number of sites and Matsubara frequencies kept in the simulation.

The accuracy of the lattice-fermionic theory in the regime where the quasiparticle bandwidth is no longer the largest energy scale requires further investigation, but, at least at the first glance, it appears to have the potential to describe many different phases, such as the polaronic metal and polaronic BCS condensate. It is interesting to understand how our theory compares to the traditional approaches to these phenomena, e.g., to those based on the Holstein-Lang-Firsov transformation [53,54].

XI. SUMMARY AND OUTLOOK

We showed in this paper that the Migdal-Eliashberg theory breaks down when the actual electron-phonon coupling λ exceeds λ_c, where $3.0 \lesssim \lambda_c \lesssim 3.7$. The breakdown is marked by negative quasiparticle heat capacity of the Migdal-Eliashberg normal state at $\lambda > 3.69$ in a range of temperatures above the superconducting transition temperature. Another pathology is the quasiparticle decay rate $\Gamma = \pi\lambda T \gg T$ at strong coupling. These findings indicate that the electron-phonon system cannot be in the state prescribed by this theory as it is thermodynamically unstable. A new phase therefore must emerge for $\lambda > \lambda_c$ below a certain critical temperature T_{c1}.

The new phase breaks the translational invariance of the crystal because strong electron-ion Coulomb interaction, $\lambda > \lambda_c$, is incompatible with uniform electron charge distribution. Instead, a lattice distortion similar to the Peierls transition occurs at λ_c that brings electrons on average closer to the ions. More precisely, this is a "many-body Peierls transition" as the electron-electron interactions mediated by quantum phonons play a critical role in it. This transition is marked by an abrupt change of the quasiparticle spectrum near the Fermi level.

We saw in our previous work [14] that solutions of Eliashberg equations correspond to stationary points of the free energy functional. The superconducting stationary point continues to exist for $\lambda > \lambda_c$ below the critical temperature T_{c2}, though it is no longer the global minimum of the free energy. We showed above that $T_{c2} < T_{c1}$ and that this implies a first-order phase transition as a function of λ between the Migdal-Eliashberg superconducting state and the new phase. Depending on the filling fraction, crystal symmetry and other parameters, the new phase can be a CDW insulator or a Fermi liquid with broken lattice translational symmetry.

We proposed a new theory—lattice-fermionic theory of superfluidity—that bridges the gap between the Migdal-Eliashberg theory and phases that emerge at stronger coupling. The idea is to incorporate the static distortion of the lattice into the single-particle Hamiltonian as a variable potential for the fermions. We treat the phonon mediated electron-electron interactions in a manner similar to the Migdal-Eliashberg theory. However, now the self-energy fields Φ_n^α, Σ_n^α, and χ_n^α depend on single-particle states $|\alpha\rangle$. The theory does not assume translational invariance. We derived the effective action for these fields and lattice distortions and determined its stationary point. The outcome is a set of

four coupled equations. Three of them are equations for the self-energies. The fourth equation is a nonlinear Schrödinger equation for the single-particle spectrum. At small λ our theory reproduces the Migdal-Eliashberg theory. Past λ_c it captures the insulating phase and at least some of the polaron physics.

An apparent open problem is to investigate the phase diagram of the lattice-fermionic theory at strong coupling and to compare it to existing studies of many-body electron-phonon physics beyond the Migdal-Eliashberg theory. Even though the equations we derived are significantly more complicated than Eliashberg equations in their simplest form, we believe our theory is nevertheless quite amenable to both computational and analytic treatments.

Note that our study implies an upper bound on the ratio of the critical temperature T_c to the characteristic phonon frequency for conventional superconductors. We use the strong coupling asymptote $T_c \approx 0.183\sqrt{\lambda}\omega_{\ln}$. Here $\omega_{\ln}$ is the characteristic bosonic frequency defined through $\ln\omega_{\ln} = \langle \ln\omega \rangle$, where $\langle \ln\omega \rangle$ is the spectral average of the log of the bosonic frequency. This formula fits T_c of superconductors with $\lambda \geqslant 2.25$ quoted in Ref. [34] reasonably well. We established above that $\lambda_c \leqslant 3.69$. It follows that $T_c/\omega_{\ln} \leqslant 0.35$, cf. upper bound proposed in Ref. [55].

ACKNOWLEDGMENT

We thank I. L. Aleiner, A. V. Chubukov, and I. V. Lerner for helpful discussions.

APPENDIX A: LOW-TEMPERATURE ENTROPY AND SPECIFIC HEAT IN $\lambda \to \infty$ LIMIT

In this Appendix, we outline the calculation of the entropy and specific heat in the superconducting state at low temperatures for $\lambda = \infty$ ($\Omega = 0$). In the main text we derived Eq. (60) for the free energy difference $\delta f = f_s - f_n$ between superconducting and normal states

$$\frac{d[\delta f]}{dT} = -8\pi\nu_0 \sum_{n=0}^{\infty}\left(\frac{\omega_n^2}{\sqrt{\omega_n^2+\Delta_n^2}} - \omega_n\right). \tag{A1}$$

It remains to evaluate the sum over the Matsubara frequencies. We do so with the help of the Poisson summation formula [56]

$$\sum_{n=0}^{\infty}\mathsf{h}(\omega_n) = \frac{1}{T}\int_0^{\infty}\mathsf{h}(\omega)\frac{d\omega}{2\pi} + \frac{\pi T}{12}\mathsf{h}'(0) - \sum_{s=1}^{\infty}\frac{2(-1)^s T}{s^2}\int_0^{\infty}\mathsf{h}''(\omega)\cos\left(\frac{\omega s}{T}\right)\frac{d\omega}{2\pi}. \tag{A2}$$

At low T, it is sufficient to keep only the $s = 1$ term in the summation over s as other terms are exponentially smaller. In our case,

$$\mathsf{h}(\omega) = \frac{\omega^2}{\sqrt{\omega^2+\Delta^2(i\omega)}} - \omega. \tag{A3}$$

We need the following two integrals,

$$I_1 = \int_0^{\infty} d\omega\left(\omega - \frac{\omega^2}{\sqrt{\omega^2+\Delta^2(i\omega)}}\right),$$
$$I_2 = -T^2\int_0^{\infty} d\omega\left(\frac{\omega^2}{\sqrt{\omega^2+\Delta^2(i\omega)}}\right)''\cos\left(\frac{\omega}{T}\right), \tag{A4}$$

where $\Delta(i\omega)$ is the solution of the $T = 0, \Omega = 0$ version of the gap equation (54),

$$\omega\sin\theta = \frac{g^2}{2}\int_{-\infty}^{\infty} d\tilde{\omega}\frac{\sin(\tilde{\theta}-\theta)}{(\omega-\tilde{\omega})^2}, \quad \theta \equiv \theta(\omega), \quad \tilde{\theta} \equiv \theta(\tilde{\omega}). \tag{A5}$$

Equations (A1) and (A2) then imply

$$\frac{df_s}{dT} = \frac{df_n}{dT} + \frac{4\nu_0 I_1}{T} + \frac{2\pi^2\nu_0 T}{3} + \frac{8\nu_0 I_2}{T}. \tag{A6}$$

Interestingly, we are able to obtain an exact answer for I_1, $4I_1 = g^2$, which can be interpreted as a sum rule that the zero temperature gap function on the Matsubara axis must satisfy in the strong coupling limit.

Recall that

$$\cos\theta(\omega) = \frac{\omega}{\sqrt{\omega^2+\Delta^2(i\omega)}}, \quad \sin\theta(\omega) = \frac{\Delta(i\omega)}{\sqrt{\omega^2+\Delta^2(i\omega)}}. \tag{A7}$$

In terms of $\theta(\omega)$, the expression for I_1 reads

$$I_1 = \int_0^{\infty} d\omega\omega(1-\cos\theta) = -\frac{1}{4}\int_{-\infty}^{\infty} d\omega\,\omega^2\theta'\sin\theta. \tag{A8}$$

Here we integrated by parts taking into account that $\Delta(i\omega)$ is even in omega and $\Delta(i\omega) \to 0$ as $\omega \to 0$ [14]. The same integral appears if we integrate the gap equation (A5) over ω and then perform integrations by parts with respect to ω on the left-hand side and with respect to both ω and $\tilde{\omega}$ on the right-hand side. We obtain

$$I_1 = \frac{g^2}{8}\int_{-\infty}^{\infty} d\omega\int_{-\infty}^{\infty} d\tilde{\omega}\frac{\omega}{\omega-\tilde{\omega}}\cos(\theta-\tilde{\theta})\theta'\tilde{\theta}'. \tag{A9}$$

Using $\omega/(\omega-\tilde{\omega}) = 1 + \tilde{\omega}/(\omega-\tilde{\omega})$, we rewrite Eq. (A9) in the form

$$I_1 = \frac{g^2}{8}\int_{-\infty}^{\infty} d\omega\int_{-\infty}^{\infty} d\tilde{\omega}\cos(\theta-\tilde{\theta})\theta'\tilde{\theta}' + \frac{g^2}{8}\int_{-\infty}^{\infty} d\omega\int_{-\infty}^{\infty} d\tilde{\omega}\frac{\tilde{\omega}}{\omega-\tilde{\omega}}\cos(\theta-\tilde{\theta})\theta'\tilde{\theta}'. \tag{A10}$$

Interchanging ω and $\tilde{\omega}$ in the last integral and comparing to Eq. (A9), we notice that it is equal to $-I_1$. Therefore

$$2I_1 = \frac{g^2}{8}\int_{-\infty}^{\infty} d\omega\int_{-\infty}^{\infty} d\tilde{\omega}\cos(\theta-\tilde{\theta})\theta'\tilde{\theta}' = \frac{g^2}{8}\int_0^{\pi} d\theta\int_0^{\pi} d\tilde{\theta}\cos(\theta-\tilde{\theta}) = \frac{g^2}{2}. \tag{A11}$$

Going back to the definition of I_1 in Eq. (A4), we see that we derived an identity

$$\int_0^\infty d\omega\left(\omega - \frac{\omega^2}{\sqrt{\omega^2+\Delta^2(i\omega)}}\right) = \frac{g^2}{4}, \tag{A12}$$

for the Eliashberg gap function $\Delta(i\omega)$ at zero temperature and $\lambda = \infty$.

Replacing $4I_1$ with g^2 in Eq. (A6) and substituting f_n from Eq. (45), we obtain the following expression for the entropy of the superconducting state:

$$S_s = -\frac{df_s}{dT} = -\frac{8\nu_0 I_2}{T}. \tag{A13}$$

Note that the second and third terms on the right-hand side of Eq. (A6) cancel the entropy of the normal state. To determine I_2, we first integrate by parts twice casting it into the form

$$\begin{aligned} I_2 &= -T^2\int_0^\infty d\omega\left(\frac{\omega^2}{\sqrt{\omega^2+\Delta^2(i\omega)}}\right)''\cos\left(\frac{\omega}{T}\right) \\ &= \frac{1}{2}\int_{-\infty}^\infty d\omega\frac{\omega^2}{\sqrt{\omega^2+\Delta^2(i\omega)}}e^{i\omega/T}. \end{aligned} \tag{A14}$$

We turn the last integral into a contour integral by closing the contour in the upper half plane of complex ω. We saw in Sec. IV C that the function $i\omega/\sqrt{\omega^2+\Delta^2(i\omega)}$ has simple poles at points where the square root vanishes [36], see also Ref. [26]. These are poles rather than branching points because roots of $\omega^2+\Delta^2(i\omega)=0$ are doubly degenerate. The poles are at a discrete set of points along the imaginary axis,

$$\omega = \pm iE_n, \quad n = 1, 2, 3, \ldots, \tag{A15}$$

where E_n are real and positive and have the meaning of single fermion energy levels. In particular, E_1 is the energy gap. This shows that the density of state is a sum of delta functions centered at E_n, i.e., the excitation spectrum is discrete in the strong coupling limit [26] provided, of course, this limit is physical in the first place.

It is now straightforward to evaluate I_2 by the residue theorem. The contribution from E_1, the pole closest to the real axis, is exponentially larger than that from all other E_n. Taking the residue at the pole and E_1 from Ref. [26], we find that the leading low-T asymptotic behaviors of the entropy S_s and the specific heat $C_s = TdS_s/dT$ are

$$\begin{aligned} S_s &\approx 17.84\nu_0\frac{E_1}{T}e^{-E_1/T}, \\ C_s &\approx 17.84\nu_0\left(\frac{E_1}{T}\right)^2 e^{-E_1/T}, \quad E_1 \approx 1.16g. \end{aligned} \tag{A16}$$

APPENDIX B: BAND STRUCTURE IN THE STRONG COUPLING REGIME

We saw in the main text that the quasiparticle spectrum is discrete in the superconducting state at $\lambda = \infty$. Here, by analyzing the gap equation on the real frequency axis, we show that at finite λ, the discrete energy levels broaden into narrow energy bands of width $\Omega = g\lambda^{-1/2}$.

In this Appendix only, we choose the energy units so that

$$g = 1, \quad \text{or, equivalently,} \quad \lambda\Omega^2 = 1. \tag{B1}$$

The Eliashberg gap equation continued towards the real axis reads [26,57,58]

$$\begin{aligned} \omega D(\omega)B(\omega) - A(\omega) = \frac{\pi}{2\Omega}\Bigg\{&\frac{D(\omega-\Omega)-D(\omega)}{\sqrt{D^2(\omega-\Omega)-1}}[n_B(\Omega) \\ &+ n_F(\Omega-\omega)] + (\Omega\to-\Omega)\Bigg\}, \end{aligned} \tag{B2}$$

where n_B and n_F are Bose and Fermi distribution functions, respectively, and

$$\begin{aligned} A(\omega) &= 2\pi T\sum_{n=0}^\infty \frac{\Delta_n\left(\omega_n^2-\omega^2+\Omega^2\right)}{X_n(\omega)\sqrt{\omega_n^2+\Delta_n^2}}, \\ B(\omega) &= 1 + 4\pi T\sum_{n=0}^\infty \frac{\omega_n^2}{X_n(\omega)\sqrt{\omega_n^2+\Delta_n^2}}, \\ D(\omega) &= \frac{\Delta(\omega)}{\omega}, \end{aligned} \tag{B3}$$

$$X_n(\omega) = \left(\omega^2+\omega_n^2\right)^2 + 2\Omega^2\left(\omega_n^2-\omega^2\right) + \Omega^4. \tag{B4}$$

Taking $T\to 0$ limit, we find

$$\omega D(\omega)B(\omega) - A(\omega) = \frac{\pi}{2\Omega}\frac{D(\omega-\Omega)-D(\omega)}{\sqrt{D^2(\omega-\Omega)-1}}. \tag{B5}$$

We are interested in the correction to the strong coupling limit $\Omega\to 0$. To obtain it, we expand the right-hand side of the above equation to the first order in Ω,

$$\frac{2}{\pi}[\omega DB - A] = \frac{D'}{\sqrt{D^2-1}} + \Omega\frac{DD'^2}{(D^2-1)^{3/2}} - \frac{\Omega}{2}\frac{D''}{\sqrt{D^2-1}}, \tag{B6}$$

where $D\equiv D(\omega)$ and $D'\equiv dD/d\omega$.

Following Combescot who used Eq. (B6) at $\Omega = 0$ to analyze the quasiparticle spectrum in the strong coupling limit [26], we introduce a new variable $\varphi(\omega)$ as $D = 1/\sin\varphi$. Eq. (B6) becomes

$$\varphi' - \frac{\Omega}{2}(\varphi'' + \varphi'^2\tan\varphi) = \frac{2}{\pi}[\omega B - A\sin\varphi]. \tag{B7}$$

The density of states (80) in terms of $\varphi(\omega)$ is

$$\nu(\omega) = \nu_0\,\mathrm{Im}[\tan\varphi(\omega)]. \tag{B8}$$

Combescot showed that $\varphi(\omega)$ is real to zeroth order in Ω, and consequently the density of states is a sum of delta functions,

$$\nu(\omega) = \pi\nu_0\sum_{k=1}^\infty P_k[\delta(\omega-E_k)+\delta(\omega+E_k)], \tag{B9}$$

where E_k are solutions of $\cos[\varphi(E_k)] = 0$, or, equivalently, of $\varphi(E_k) = \pi(k-1/2)$. Imaginary part of $\nu(\omega)$ comes from poles of $\tan\varphi(\omega)$ at $\omega = \pm E_k - i0^+$. It is straightforward to show using Eq. (B3) that $A(\omega)$ vanishes as $1/\omega^2$ and $B(\omega)\to 1$ as $\omega\to\infty$. At $\Omega = 0$ and large ω, Eq. (B7) takes the form $\varphi' = 2\omega/\pi$. Therefore $\varphi(\omega)\approx\omega^2/\pi\equiv\varphi_0(\omega)$ which implies the leading large k asymptotic behavior (82) of E_k.

Let us analyze Eq. (B7) at large ω and small but finite Ω. Corrections to the right-hand side due to finite Ω are suppressed by a factor of $1/\omega^2$. In the zeroth order in Ω, $\varphi'\sim\omega$

and $\varphi'' \sim 1$. Therefore the term containing φ'' is negligible and we have

$$\varphi' - \frac{\Omega}{2}\varphi'^2 \tan\varphi = \frac{2\omega}{\pi}. \tag{B10}$$

The $\tan\varphi$ term is important near $\omega = E_k$ where $\tan\varphi$ diverges. Near these points Eq. (B10) becomes

$$y' + \frac{\Omega}{2}\frac{y'^2}{y} = \frac{2E_k}{\pi}, \tag{B11}$$

where $y = \varphi(\omega) - \varphi_0(E_k) = \varphi(\omega) - E_k^2/\pi$. Solving for y', we find

$$y' = -\frac{1}{\Omega}(y + \sqrt{y^2 + by}), \quad b = \frac{8\Omega E_k}{\pi}. \tag{B12}$$

The plus sign is dictated by the requirement that for $\Omega \to 0$ we recover the zeroth-order equation $y' \approx 2E_k/\pi$. In zeroth order in Ω, $y = 2\omega E_k/\pi$ is real and the density of states (B8) is zero except at $\omega = E_k$ In the next order in Ω, y and therefore $\varphi(\omega)$ acquire an imaginary part proportional to Ω. We see this from Eq. (B12)—the square root is imaginary and of the order Ω for $-b < y < 0$. Upon integration over ω, it gives rise to an imaginary part of y of the order Ω. The density of states (B8) is therefore nonzero in the interval (ω_1, ω_2) of ω for which y falls in between $-b$ and 0. The length of this interval is the bandwidth we are after.

Equation (B12) integrates by variable separation method to

$$\frac{b}{u(y)} - \frac{1}{2}\ln u^2(y) = \frac{2\omega}{\Omega} + \text{const}, \tag{B13}$$

$$u(y) = b + 2y + \sqrt{y^2 + by}. \tag{B14}$$

To determine ω_1 and ω_2, we set $y = -b$ and $y = 0$, respectively, in the left-hand side of Eq. (B13). We find $\omega_2 - \omega_1 = \Omega$. Thus the discrete level E_k splits into a narrow band of width Ω similar to how atomic energy levels split into bands when atoms form a lattice and atomic orbitals hybridize.

[1] A. B. Migdal, Interaction between electrons and lattice vibrations in a normal metal, Sov. Phys. JETP **34**, 996 (1958) [J. Exptl. Theoret. Phys. (U.S.S.R.) **34**, 1438 (1958)].

[2] G. M. Eliashberg, Interactions between electrons and lattice vibrations in a superconductor, Sov. Phys. JETP **11**, 696 (1960) [J. Exptl. Theoret. Phys. (U.S.S.R.) **38**, 1438 (1960)].

[3] J. Bardeen, L. N. Cooper, and J. R. Schrieffer, Theory of superconductivity, Phys. Rev. **108**, 1175 (1957).

[4] L. D. Landau and E. M. Lifshitz, *Statistical Physics, Part 1* (Butterworth-Heinemann, 1980), 3rd ed.

[5] A. J. Millis, R. Mueller, and B. I. Shraiman, Fermi-liquid-to-polaron crossover. I. General results, Phys. Rev. B **54**, 5389 (1996).

[6] P. Benedetti and R. Zeyher, Holstein model in infinite dimensions at half-filling, Phys. Rev. B **58**, 14320 (1998).

[7] A. S. Alexandrov, Breakdown of the Migdal-Eliashberg theory in the strong-coupling adiabatic regime, Europhys. Lett. **56**, 92 (2001).

[8] D. Meyer, A. C. Hewson, and R. Bulla, Gap Formation and Soft Phonon Mode in the Holstein Model, Phys. Rev. Lett. **89**, 196401 (2002).

[9] M. Capone and S. Ciuchi, Polaron Crossover and Bipolaronic Metal-Insulator Transition in the Half-Filled Holstein Model, Phys. Rev. Lett. **91**, 186405 (2003).

[10] I. Esterlis, S. A. Kivelson, and D. J. Scalapino, Pseudogap crossover in the electron-phonon system, Phys. Rev. B **99**, 174516 (2019).

[11] I. Esterlis, B. Nosarzewski, E. W. Huang, B. Moritz, T. P. Devereaux, D. J. Scalapino, and S. A. Kivelson, Breakdown of the Migdal-Eliashberg theory: A determinant quantum Monte Carlo study, Phys. Rev. B **97**, 140501(R) (2018).

[12] J.-P. Pouget, The Peierls instability and charge density wave in one-dimensional electronic conductors, C. R. Phys. **17**, 332 (2016).

[13] S. van Smaalen, The Peierls transition in low-dimensional electronic crystals, Acta Crystallogr. A **61**, 51 (2005).

[14] E. A. Yuzbashyan and B. L. Altshuler, Migdal-Eliashberg theory as a classical spin chain, Phys. Rev. B **106**, 014512 (2022).

[15] V. V. Kabanov and O. Yu. Mashtakov, Electron localization with and without barrier formation, Phys. Rev. B **47**, 6060 (1993).

[16] A. A. Abrikosov, L. P. Gorkov, and I. E. Dzyaloshinski, *Methods of Quantum Field Theory in Statistical Physics* (Dover, New York, 1975).

[17] There is a factor of 2 difference between Migdal's and Eliashberg's definition [1,2] of λ_0 and the modern definition which we are using, $2\lambda_0|_{\text{our}} = \lambda_0|_{\text{ME}}$, so that Migdal and Eliashberg's $\lambda_0 \lesssim 1$ becomes $\lambda_0 \lesssim 0.5$ as in Ref. [16], pp. 78 and 181.

[18] E. A. Yuzbashyan and B. L. Altshuler, Fluctuations in boson mediated superconductors and the meaning of the Migdal theorem (tentative title) (unpublished).

[19] A. V. Chubukov, A. Abanov, I. Esterlis, and S. A. Kivelson, Eliashberg theory of phonon-mediated superconductivity: When it is valid and how it breaks down, Ann. Phys. **417**, 168190 (2020).

[20] P. B. Allen and R. C. Dynes, Transition temperature of strong-coupled superconductors reanalyzed, Phys. Rev. B **12**, 905 (1975).

[21] E. G. Brovman and Yu. Kagan, The phonon spectrum of metals, Sov. Phys. JETP **25**, 365 (1967) [J. Exptl. Theoret. Phys. (U.S.S.R.) **52**, 557 (1967)].

[22] B. T. Geĭlikman, Adiabatic perturbation theory for metals and the problem of lattice stability, Sov. Phys. Usp. **18**, 190 (1975).

[23] I. S. Tupitsyn, A. S. Mishchenko, N. Nagaosa, and N. Prokof'ev, Coulomb and electron-phonon interactions in metals, Phys. Rev. B **94**, 155145 (2016).

[24] P. B. Allen and B. Mitrovic, Theory of superconducting T_c, in *Solid State Physics*, edited by H. Ehrenreich, F. Seitz, and D. Turnbull (Academic, New York, 1982), Vol. 37, p. 1.

[25] F. Marsiglio and J. P. Carbotte, Electron-phonon superconductivity, in *Superconductivity*, edited by K. H. Bennemann and J. B. Ketterson (Springer, Berlin, Heidelberg, 2008).

[26] R. Combescot, Strong-coupling limit of Eliashberg theory, Phys. Rev. B **51**, 11625 (1995).

[27] E. A. Yuzbashyan, M. K.-H. Kiessling, and B. L. Altshuler, Superconductivity near a quantum critical point in the extreme retardation regime, Phys. Rev. B **106**, 064502 (2022).

[28] We dub f the free energy even though it is, strictly speaking, the grand potential as it is a function of the chemical potential rather than the particle number.

[29] P. W. Anderson, Random-phase approximation in the theory of superconductivity, Phys. Rev. **112**, 1900 (1958).

[30] G. Grimvall, *The Electron-Phonon Interaction in Metals* (North-Holland, 1981), p. 125.

[31] A usual way to derive this is to use the Poisson summation formula discarding the divergent ground state energy. It is worthwhile to note that the zeta function regularization procedure [32] leads to the same result. Using $\omega_n = 2\pi T(n + \frac{1}{2})$, we have $f = -4\pi\nu_0 T^2 \sum_{n=-\infty}^{\infty} |n + \frac{1}{2}|$. Further, $\sum_{n=-\infty}^{\infty} |n + \frac{1}{2}| = 2\zeta(-1, \frac{1}{2}) = \frac{1}{24}$, where $\zeta(s, a)$ is the Hurwitz zeta function, and Eq. (32) follows.

[32] H. Kleinert, *Path Integrals in Quantum Mechanics, Statistics, Polymer Physics, and Financial Markets* (World Scientific, 2009).

[33] This divergence cannot be removed by zeta function regularization, because $\zeta(s)$ is singular at $s = 1$.

[34] J. P. Carbotte, Properties of boson-exchange superconductors, Rev. Mod. Phys. **62**, 1027 (1990).

[35] M. Kiessling, E. A. Yuzbashyan, and B. L. Altshuler (unpublished).

[36] Note that ω in Sec. IV C differs from ω in Appendix A and Eq. (61) by a factor of i.

[37] F. Marsiglio and J. P. Carbotte, Gap function and density of states in the strong-coupling limit for an electron-boson system, Phys. Rev. B **43**, 5355 (1991).

[38] G. D. Mahan, *Many-Particle Physics*, 3rd ed. (Springer, Boston, MA, 2000).

[39] E. A. Yuzbashyan, A. A. Baytin, and B. L. Altshuler, Strong-coupling expansion for the pairing Hamiltonian for small superconducting metallic grains, Phys. Rev. B **68**, 214509 (2003).

[40] H. A. Kramers, Brownian motion in a field of force and the diffusion model of chemical reactions, Physica **7**, 284 (1940).

[41] P. Hänggi, P. Talkner, and M. Borkovec, Reaction-rate theory: Fifty years after Kramers, Rev. Mod. Phys. **62**, 251 (1990).

[42] V. I. Mel'nikov, The Kramers problem: Fifty years of development, Phys. Rep. **209**, 1 (1991).

[43] P. A. Lee and T. V. Ramakrishnan, Disordered electronic systems, Rev. Mod. Phys. **57**, 287 (1985).

[44] P. W. Anderson, Theory of dirty superconductors, J. Phys. Chem. Solids **11**, 26 (1959).

[45] O. V. Dolgov, O. K. Andersen, and I. I. Mazin, Self-consistent theory of phonon renormalization and electron-phonon coupling near a two-dimensional Kohn singularity, Phys. Rev. B **77**, 014517 (2008).

[46] E. Maksimov and D. Khomskii, The electron-phonon interaction in metals and the problem of lattice stability, in *High temperature Superconductivity*, edited by V. Ginzburg and D. Kirzhnits (Consultants Publisher, New York, 1982).

[47] J. Bauer, J. E. Han, and O. Gunnarsson, Quantitative reliability study of the Migdal-Eliashberg theory for strong electron-phonon coupling in superconductors, Phys. Rev. B **84**, 184531 (2011).

[48] For an insulator ν_0 can be defined, e.g., as the density of states averaged over the valence band.

[49] This algebra implies that translations of the set $\{x_i\} \to \{x_{i+\boldsymbol{m}}\}$ for any $\boldsymbol{m}$ are also eigenstates with the same energy. The degree of the degeneracy is the number of inequivalent sets that such translations generate. For example, the configuration $x_i = X_{\text{c.m.}} + (-1)^{i_x+i_y}\delta x$ on a square lattice is twofold degenerate.

[50] Y. Ono and T. Hamano, Peierls distortion in two-dimensional tight-binding model, J. Phys. Soc. Jpn. **69**, 1769 (2000).

[51] However, the (π, π) variational wave function is suboptimal away from half filling, so the true λ_0^c must be smaller.

[52] Y. Suzuki, Small bipolaron conductivity in the Holstein-Hubbard Model, J. Phys. Soc. Jpn. **66**, 306 (1997).

[53] A. S. Alexandrov, Many-body effects in the normal-state polaron system, Phys. Rev. B **46**, 2838 (1992).

[54] T. Holstein, Studies of polaron motion: Part II. The "small" polaron, Ann. Phys. **8**, 343 (1959).

[55] I. Esterlis, S. A. Kivelson, and D. J. Scalapino, A bound on the superconducting transition temperature, npj Quantum Mater. **3**, 59 (2018).

[56] G. Grosso and G. Parravicini, *Solid State Physics*, 2nd ed. (Academic Press, 2013).

[57] F. Marsiglio, M. Schossmann, and J. P. Carbotte, Iterative analytic continuation of the electron self-energy to the real axis, Phys. Rev. B **37**, 4965 (1988).

[58] A. E. Karakozov, E. G. Maksimov, and A. A. Mikhailovsky, The investigation of Eliashberg equations for superconductors with strong electron-phonon interaction, Solid State Commun. **79**, 329 (1991).